TWO PHASE FLOW IN CAPILLARY TUBE

Mikio Suo
Peter Griffith

March, 1963

Report No. 8581-24
Department of Mechanical Engineering
Massachusetts Institute of Technology

Contract No. AF 19(604)-7344

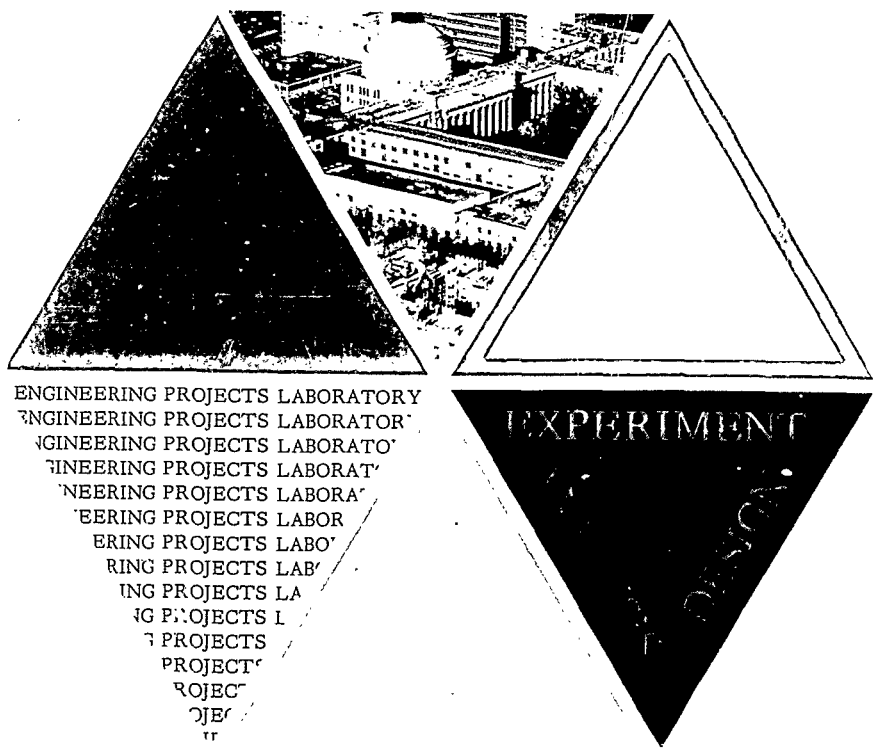

TWO PHASE FLOW IN CAPILLARY TUBES

by

Mikio Suo
Peter Griffith

TECHNICAL REPORT NO. 8581-24

Massachusetts Institute of Technology
National Magnet Laboratory

Sponsored by the Solid State Sciences Division
Air Force Office of Scientific Research (OAR)
Air Force Contract AF 19(604)-7344

Department of Mechanical Engineering
Massachusetts Institute of Technology
Cambridge 39, Massachusetts

ACKNOWLEDGEMENTS

This project was supported in part by the National Magnet Laboratory at the Massachusetts Institute of Technology. The National Science Foundation provided financial assistance to one of the authors for the period in which the work was done.

The authors are indebted to Doctor F. B. Bretherton for assistance in guiding the work in its early stages.

ABSTRACT

The flow of two phases, gas and liquid, has been studied in horizontal tubes of capillary diameter. The flow has been primarily studied in the regime where the gas flows as long bubbles separated from the wall of the tube by a liquid film and from each other by slugs of liquid. In this regime the pressure drop, density and, to a certain extent, the thickness of the liquid film around a bubble have been correlated. The conditions under which the long bubble flow can exist and under which the correlations are valid have been determined. Of special interest is that the correlations should be valid in a zero gravity field.

TABLE OF CONTENTS

1. INTRODUCTION

The study of two phase flow is assuming a greater and greater importance in the technologies of heat transfer and fluid mechanics. Unfortunately, there is no simple way to analyze or correlate all types of two phase flow problems. A large amount of effort must be expended on categorizing each type of flow problem and analyzing and correlating the significant parameters of each type. This work categorizes one type of flow problem and analyzes and correlates the significant parameters of it.

As the title would indicate, the problem to be studied here concerns two phase flow in tubes of capillary diameter. More specifically, the problem is concerned with flows which have long, somewhat symmetrical gas bubbles separated from the wall of the tube with a liquid film and separated from each other with liquid slugs. The flow geometry or flow regime described occurs quite often in capillary tubes. Because of its similarity to the slug flow regime in large tubes and because of the small tube diameters, the flow regime is called capillary slug flow. To give an idea of the order of magnitude of the size of the systems dealt with here, it can be said that the work concerns tubes in the order of one millimeter in diameter and velocities up to around ten feet per second.

The problem first came up in the study of boiling in small tubes for high intensity magnets. It was thought that the two phase flow in these tubes could be analyzed in a simpler manner than the common two phase flow problem in larger tubes. Capillary slug flow was not necessarily the only flow regime observed in these tubes, but study of this flow regime was thought to be a good place to start the problem. Other places where capillary slug flow may occur is in refrigerators and possibly in spacecraft boilers and condensers. The latter use stems from the idea that in capillary tubes the effects of gravity should be negligible on earth and correlations for them should be valid at zero gravity.

Some work has been done on the problem of capillary slug flow. In general, the previous work falls into two groups. One group has measured pressure drop or film thickness at very low Reynolds Numbers where the inertia forces are very small. Their observations were made using glass tubes where the bubbles were observed to exist. The other group has measured pressure drop and over-all mixture density at higher Reynolds Numbers. They did not observe or at least

did not report whether the bubbles actually existed. Of the former group, there are Fairbrother and Stubbs[6+], F. Bretherton[4], G. I. Taylor[19], Marchessault and Mason[14] and Goldsmith and Mason[7]. Of the latter group, there are Lockhart and Martinelli[13], G. P. Marcy[15], and H. A. Whitesel[20]. These groups have obtained satisfactory answers to the problem of film thickness at very low Reynolds Numbers. They have not obtained satisfactory answers to film thickness or over-all density at higher Reynolds Numbers (inertia not negligible compared to viscosity). Nor have they obtained satisfactory answers to pressure drop at any Reynolds Numbers.

In most of the previous work the flow was studied with horizontal tubes. In this work the flows are horizontal also. The flow regime should properly be called capillary slug flow in horizontal tubes. Where there is no chance of confusion, the flow may simply be called slug flow.

The pressure drop, density and film thickness are studied for a certain type of horizontal capillary slug flow. The existence of this type of flow (flow regime study) is studied also. The type of flow is one where the surface tension forces are large compared to the gravity forces and the liquid viscosity and density are large compared to the gas viscosity and density. The flow is studied with gas and liquid rather than vapor and liquid. Compressible effects are ignored to a large extent as is heat addition.

[+]Superscript numbers are referred to in the Bibliography.

2. ANALYSIS OF FLOW

2.1. Flow Model

Several questions come to mind for a flow model. The prime question is whether the slug flow regime is stable. That is, do the bubbles tend to stay discrete or do they tend to agglomerate. If the bubbles tend to agglomerate, an analytical flow model becomes quite difficult.

To determine whether bubbles and slugs of various lengths tend to agglomerate a preliminary test apparatus was constructed. This apparatus showed that long bubbles do not tend to agglomerate. The bubbles appeared to stay at constant length and travel at the same velocity as others in the tube. There were some variations in bubble velocities but they were small compared to the total velocities. If a small bubble (1-2 diameters) occurred, there would be agglomeration of the long bubbles behind the small bubble until the small bubble agglomerated also; then no further agglomeration would take place.

These experiments indicate that a model without agglomeration would be a reasonable one for slug flow. The problem is still quite difficult because of the infinite number of possible combinations of bubble and slug lengths. The problem is considerably simplified if a model is taken for analysis and experiment which has all the bubbles of one length and all the slugs of another. All the bubbles travel at the same velocity and remain constant in length as they flow through the tube. The model can be viewed from two viewpoints. If one looks at the whole tube, one sees a group of bubbles and slugs all of the same length with all the bubbles traveling at the same velocity. This picture is steady in time. On the other hand, one may stand on a point in the tube and watch bubbles and slugs go by. Each bubble and slug passing the point has the same length as the others before and after it and each bubble has the same velocity. The bubble and slug lengths and bubble velocity do not change as they go down the tube. This model would appear to be a reasonable one if the end effects can be neglected. In long tubes this seems a reasonable assumption. Initial experiments indicated that this type of flow is also possible and therefore the flow is analyzed in this manner. It is explained where required how to extend the results of this type of analysis to the case where bubbles and slugs are not uniform.

The uniform bubble and slug length model is as shown in Fig. 2. In addition to uniform bubble and slug lengths, several more requirements are made on the model.

The first requirement is that the gas and liquid are both incompressible. The second requirement is that the liquid to gas density and viscosity ratios are much greater than one. That is:

$$\frac{\rho_l}{\rho_g} \gg 1 \tag{1}$$

$$\frac{\mu_l}{\mu_g} \gg 1 \tag{2}$$

The first requirement restricts us to relatively small pressure drops. The second requirement restricts us very little as this is most often the case with liquid-gas systems. It does simplify the problem considerably because it causes the bubbles to be constant pressure volumes imbedded in the liquid.

2.2. Dimensional Analysis

A complete analysis of the flow might appear possible from the geometry of the model. However, it turns out to be very difficult, if indeed not impossible. An analysis has been made for film thickness by Bretherton[4] in the case of non-inertial flow. To go beyond this to the case where inertial forces are important, then to the point where the flow is turbulent, would require an inordinate amount of work. For this reason, a dimensional analysis is performed to determine what parameters are required to determine the flow.

The Navier-Stokes equations will yield the proper dimensionless groups for the liquid. They can be several different combinations, but two which are common are the Froude Number and the Reynolds Number:

$$N_{Fr} = \frac{V^2}{gL} \tag{3}$$

$$N_{Re} = \frac{\rho_l V L}{\mu_l} \tag{4}$$

where V is some characteristic velocity and L is some characteristic length.

The boundary conditions at the gas-liquid interface will yield one additional dimensionless group which must be given in terms of the surface tension and other forces. This can be derived either using the Pi theorem or by examining the differential equations of the liquid at the interface. One combination which turns out to be particularly useful is:

$$\lambda = \frac{\mu_l^2}{\rho_l \sigma r_o} \tag{5}$$

The utility of λ is that it is not dependent on any velocity. It is a property of a given system. Thus controlling this parameter is quite simple.

The dimensionless groups above contain an arbitrary velocity and an arbitrary length. The arbitrary length is chosen to be r_o, the tube radius, because of simplicity. The choice of velocity is not quite so easy to make. As will be seen later, the average velocity U_S of the liquid in a slug is very simple and characteristic, but on the other hand, the bubble velocity U_B is characteristic also. The bubble velocity in fact turns out to correlate the data in the simplest manner so it is used.

In addition to the parameters (3), (4), and (5) something must be said of the geometry to completely specify the flow. The only geometric variables we have are the bubble and slug lengths. These two in the dimensionless forms (L_B/r_o) and (L_S/r_o) together with parameters (3), (4), and (5) specify the geometry exactly. In doing so, they also specify the flow completely.

Since the shapes of the bubbles are now specified, the volume flow rates of liquid and gas are specified also. It can be seen that the process could have been reversed. The gas and liquid flow rate ratio could have been specified plus inlet conditions to give certain size bubbles. This latter technique is more difficult in this case and is not used; however, it proves a useful way of specifying a flow later on.

This method of dimensional analysis using the differential equations and some physical insight has been used because it gives an appreciation of where each parameter comes from. It could have been done equally well by simply taking all the parameters involved and using the Pi theorem.

2.3. Reduction of Parameters

Parameters (3), (4), and (5) plus (L_B/r_o) and (L_S/r_o) specify a system as shown in Fig. 2 under a great number of possible conditions. If some of the possible conditions can be eliminated, some of the five parameters can be eliminated.

One condition which can be eliminated is the effect of the gravitational forces. It would seem reasonable that one of the conditions for the capillary slug flow regime to exist is that the gravitational forces are small compared to the surface tension forces. We have no direct measure of this ratio of forces in parameters (3), (4), and (5). They can be combined to obtain this ratio of forces, however. The parameter Ω, the ratio of gravitational forces to surface tension forces, is obtained from (3), (4), and (5) as:

$$\Omega = \frac{\rho_\ell g r_o^2}{\sigma} \tag{6}$$

If this parameter is sufficiently small, the effect of gravity on the curvature of the bubble should be small.

Gravity may affect the flow in another way. It may cause the bubble to rise to the top of the tube. This depends on the viscous and inertial forces also.

The complete solution of the shape of the bubble depends on the interactions of all these forces. To make the problem tractable let us assume that if Ω is sufficiently small, then the bubble will be symmetrical about the centerline of the tube and the effect of gravity can be completely neglected. This is a major requirement and a priori we have no real reason to assume that it is valid. The ways in which this assumption may be checked are discussed in Sec. 2.9.

Since the gravity forces are neglected, the Froude Number need no longer be specified. We can go one step further than this in the elimination of parameters. To do this we make use of some experimental observations.

Under the condition of small Ω , bubbles have been found to exist as long cylindrical bubbles with little axial curvature except at the nose and tail. This observation allows us to eliminate the bubble length as a parameter to a large extent.

The lack of curvature in the bubbles means that the bubbles have a constant radius r_B. The pressure in the liquid film can then be written as:

$$p_f = p_B - \frac{\sigma}{r_B} \tag{7}$$

p_B is a constant so p_f must be a constant also. Therefore, there is no pressure drop in the liquid film. This leads to the conclusion that there is no flow in the liquid film. If there is no flow in the liquid film, it must be laid down at the nose of the bubble and then stay at that thickness until the tail of the bubble comes past. The observation of a constant bubble radius appears consistent with a bubble nose continually laying down a film of some given thickness.

Since there is no pressure drop along the cylindrical portion of the bubble, the length of the bubble must have no effect on the pressure drop associated with one bubble and slug. It would of course affect the pressure gradient. The film thickness is also not affected by the bubble length. It should make no difference to the nose of the bubble how long the cylindrical section is since the nose effectively sees only the film immediately adjacent to it and that portion is always standing still.

These arguments show that only three parameters are required to correlate pressure drop and film thickness. They are:

$$N_{Re} = \frac{\rho_l U_B r_o}{\mu_l} \tag{8}$$

$$\lambda = \frac{\mu_l^2}{\rho_l \sigma r_o} \tag{9}$$

$$\frac{L_S}{r_o} \tag{10}$$

A fourth parameter (L_B/r_o) must still be considered necessary for complete specification of the flow.

2.4. Continuity Relationships

Several relationships exist which simplify the method of attack. Two of these are derived here for later use.

The first relationship is one to determine the average velocity of the liquid in a slug. To do this we take a flow model as shown on Fig. 3. The flow is a slug flow with no restrictions except that the two phases must be incompressible. This flow is not necessarily capillary slug flow but may be. The gas and liquid may come together in some arbitrary manner. A control volume is drawn around the pipe as shown by the dotted line. It intersects the gas and liquid inlet lines prior to the point where the two phases mix.

The mass continuity relationships may be written for the two phases as follows:

$$Q_{g1}\rho_g - Q_{g2}\rho_g = \frac{d}{dt}\left(\mathcal{V}_{gc.v.}\,\rho_g\right) \tag{11}$$

$$Q_{\ell 1}\rho_\ell - Q_{\ell 2}\rho_\ell = \frac{d}{dt}\left(\mathcal{V}_{\ell c.v.}\,\rho_\ell\right) \tag{12}$$

From the fact that the control volume remains constant, we may say:

$$\frac{d}{dt}\,\mathcal{V}_{\ell c.v.} = -\frac{d}{dt}\,\mathcal{V}_{gc.v.} \tag{13}$$

Equations (11), (12) and (13) can be combined to get:

$$Q_{\ell 2} + Q_{g2} = Q_{g1} + Q_{\ell 1} \tag{14}$$

The location of the exit from the control volume is arbitrary. Therefore, equation (14) states that the total volume flow at any point in the tube is equal to the sum of the inlet volume flow rates. This is not surprising, but the next step yields an interesting result. If the exit from the control volume is located across a slug, then Q_{g2} is equal to zero. Then $Q_{\ell 2}$ is equal to the sum of the inlet gas and liquid flow rates Q_{g1} and $Q_{\ell 1}$. This should be so for all slugs.

Therefore, at any given time the volume flow rate of liquid in all slugs is the same and is given by the relation:

$$Q_S = Q_{\ell 1} + Q_{g1} \tag{15}$$

The average liquid velocity in a slug is defined as the volume flow rate of liquid divided by the tube cross-sectional area. Thus we can say that:

$$U_S = \frac{Q_{g1} + Q_{\ell 1}}{\pi r_o^2} \tag{16}$$

It is shown in Sec. 2.6 that if U_B is constant in time under the conditions of Secs. 2.1, 2.2, and 2.3, then U_S is constant in time also. This means that $(Q_{g1} + Q_{\ell 1})$ must remain constant in time. The inlet flow rates may vary but their sum must remain constant. It can be shown that no matter what the bubble-slug spacing may be, if the sum $(Q_{g1} + Q_{\ell 1})$ is constant in time, it is equal to the sum of the average gas and liquid flow rates $Q_\ell + Q_g$. Thus we can say:

$$U_S = \frac{Q_\ell + Q_g}{\pi r_o^2} \tag{17}$$

This will in general be the velocity called slug velocity. Notice that this is not the velocity at which a slug is seen moving. The slug will move along at the velocity of the bubbles U_B. U_S is the average velocity of the liquid in a slug as seen by an observer standing on the tube.

The second relationship involves the liquid in the slug also. It is a relationship for the amount of liquid which will pass a fixed point in the tube during the time that one bubble and one slug go by. To derive this relationship use will be made of the flow model of Fig. 2. The restrictions of Secs. 2.1, 2.2, and 2.3 must hold in this particular case. If we stand at a point where at time zero the tail of a bubble passes by, we see fluid flowing past at the rate $(U_S \pi r_o^2)$. This

flow lasts for a period of time approximately equal to (L_S/U_B). The flow of liquid stops when the bubble comes by. Thus we can write an equation for the volume of liquid going past our fixed point during the time it takes for one bubble and one slug to go past as:

$$\mathcal{V}_S = U_S \pi r_o^2 \frac{L_S}{U_B} \tag{18}$$

This can be rearranged to give:

$$\frac{\mathcal{V}_S}{\pi r_o^3} = \frac{U_S}{U_B} \frac{L_S}{r_o} \tag{19}$$

This relation proves to be useful later on. It is a measure of slug length and is considerably easier to measure than slug length.

2.5. Pressure Drop

The total pressure drop in a system can be given in terms of the pressure drop associated with each bubble and slug. This pressure drop per bubble and slug is more convenient than pressure gradient. The pressure drop per bubble and slug should be independent of bubble length for a constant pressure bubble, whereas the pressure gradient should not.

According to the preceding sections of this chapter the pressure drop per bubble and slug may be correlated as a function of N_{Re}, λ and $(\mathcal{V}_S/\pi r_o^3)$. An exact analytical solution is not available or very possible but some fairly simple analysis beyond the dimensional analysis is helpful to see how to plot the data.

It is reasonable that when the flow is slow enough to give a low value of N_{Re}, there is a portion of the flow in a slug which is fully developed laminar flow. The ends of the bubbles may cause some effects on the slugs. At low N_{Re} the end effects should not extend into the slugs very far. As long as the end effects do not go far enough into the slugs to disrupt the fully developed laminar flow, the end effects should be completely independent of slug length. Thus we could write the pressure drop in a bubble and slug as a linear combination of two terms:

$$\Delta P = 8\left(\frac{\mu_\ell U_S}{r_o}\right)\left(\frac{L_S}{r_o}\right) + K \tag{20}$$

where the first term on the right is the laminar flow pressure drop and K is the end effect. Equation (19) can be used to rearrange equation (20) to:

$$\frac{\Delta P}{\frac{\mu_\ell U_B}{r_o}} = \frac{8\mathcal{V}_S}{\pi r_o^3} + K \tag{21}$$

K is not the same in both equation (20) and (21), of course. It simply represents end effects of some kind. The K may be a function of N_{Re} and λ, but by definition not of (L_S/r_o) or $(\mathcal{V}_S/\pi r_o^3)$.

The range of validity of equation (21) and the function K must both be determined by experiment. Outside the range of equation (21) no simple analysis is available. There we can only use the dimensional analysis to guide the experiments. This is still not too bad. The three variables N_{Re}, λ, and $(\mathcal{V}_S/\pi r_o^3)$ should not be difficult to vary independently.

Correlations based on $(\mathcal{V}_S/\pi r_o^3)$ and derived from uniform bubble and slug lengths should apply to the case of nonuniform bubble and slug lengths provided that the film thicknesses of all bubbles in a tube are approximately constant.

2.6. Density of Mixture

The ratio of the volume of gas to the volume of liquid in a tube is not necessarily the ratio of the gas flow rate to the liquid flow rate. Therefore density, which is determined from the ratio of gas to liquid in a tube, is difficult to calculate in general. In a slug flow, however, we have a simple means of determining density.

To show how density may be determined, we once again take the flow model of Fig. 2. The average density of one bubble and one slug can be defined as:

$$\rho = \frac{\rho_\ell \left[\pi r_o^2 \left(L_S + L_B\right) - \mathcal{V}_B\right] + \rho_g \mathcal{V}_B}{\pi r_o^2 \left(L_S + L_B\right)} \tag{22}$$

where $\mathcal{V}_B$ is the bubble volume. This can be reduced to:

$$\rho = \rho_\ell + \frac{\mathcal{V}_B \left(\rho_g - \rho_\ell\right)}{\pi r_o^2 \left(L_S + L_B\right)} \tag{23}$$

The volume of gas in each bubble can be stated as:

$$\mathcal{V}_B = \frac{Q_g \left(L_S + L_B\right)}{U_B} \tag{24}$$

Equations (23) and (24) can be combined with Equation (17) to give:

$$\rho = \rho_\ell - \left(\rho_\ell - \rho_g\right) \left(\frac{Q_g}{Q_g + Q_\ell}\right) \left(\frac{U_S}{U_B}\right) \tag{25}$$

This equation is exact and depends only on continuity relationships and the definition of average density. If we make the restriction that $(\rho_\ell / \rho_g) >> 1$, then equation (25) reduces to:

$$\rho = \rho_\ell \left[1 - \left(\frac{Q_g}{Q_g + Q_\ell}\right) \left(\frac{U_S}{U_B}\right)\right] \tag{26}$$

This equation gives the average density over any integral number of bubbles.

A quite similar equation for density was derived by Griffith and Wallis. They developed density in terms of velocity differences instead of velocity ratio.

Equation (26) can be extended to the case where the bubbles and slugs are not of uniform length. The only requirements are that all the bubbles have the same velocity and that the flow rates of gas and liquid do not fluctuate sharply. By the latter it is meant that in the time it takes for a bubble to pass through the tube, the flow coming out the end of the tube should average out to the average gas and liquid flow rates. The analysis for density is performed using the model of Fig. 4. Ignoring gas density, the average density in L_t should be:

$$\rho = \frac{\rho_\ell \left[\pi r_o^2 L_t - \sum_{i=1}^{n} \mathcal{V}_{Bi} \right]}{\pi r_o^2 L_t} \tag{27}$$

Equation (27) can be reduced to:

$$\rho = \rho_\ell \left[1 - \frac{\sum_{i=1}^{n} \mathcal{V}_{Bi}}{\pi r_o^2 L_t} \right] \tag{28}$$

From the restriction that the flow rates do not vary sharply from the average it can be said that:

$$Q_g = \left(\sum_{i=1}^{n} \mathcal{V}_{Bi} \right) \frac{U_B}{L_t} \tag{29}$$

Equations (28), (29) and (17) can be combined to give:

$$\rho = \rho_\ell \left[1 - \left(\frac{Q_g}{Q_g + Q_\ell} \right) \left(\frac{U_S}{U_B} \right) \right] \tag{30}$$

It is seen that equation (30) is exactly the same as (26)

The density over a whole tube should not be significantly different from the density over an integral number of bubbles. This is especially true when the number of bubbles in a tube is large.

From equations (26) and (30) it is seen that to correlate density we need only correlate (U_S/U_B). In the flow model of uniform bubble and slug lengths this can only be a parameter of N_{Re}, λ, $(\mathcal{V}_S/\pi r_o^3)$ and (L_B/r_o). It is shown in the next section that the independence of film thickness on bubble length also implies independence of (U_S/U_B) on bubble length. Thus (L_B/r_o) can be disregarded as a parameter. The model of uniform bubbles and slugs was chosen because bubble velocity and thus (U_S/U_B) were thought to be independent of slug length or $(\mathcal{V}_S/\pi r_o^3)$. We cannot entirely disregard $(\mathcal{V}_S/\pi r_o^3)$ in correlating (U_S/U_B) but its effects should be small.

2.7. Film Thickness

The film thickness is related to the bubble and slug velocities by the relationship:

$$\frac{U_S}{U_B} = 1 - m \tag{31}$$

where m is the fraction of the cross-sectional area of the tube covered with liquid. For a concentric bubble m is given by:

$$m = 1 - \left(\frac{r_B}{r_o}\right)^2 \tag{32}$$

where r_B is the bubble radius. This relationship results from continuity and the lack of flow in the liquid film. The volume flow at a cross-section intersecting a bubble is equated to the volume flow at a cross-section intersecting a slug as follows:

$$U_B(1 - m)\,\pi r_o^2 = U_S\,\pi r_o^2 \tag{33}$$

From (33) equation (31) follows.

Equation (31) implies that if film thickness is not affected by bubble length, neither is the ratio of slug to bubble velocity.

If the bubble length stays constant, then the film thickness as measured by (1 - m) must remain constant. Thus the model of constant bubble length and constant bubble velocity implies constant U_S.

2.8. Effect of Gas Viscosity

The analysis for the most part has had one restriction on the viscosity of the gas which is that the viscosity ratio (μ_ℓ / μ_g) must be much greater than one. It has not yet been established, however, how a finite gas viscosity will effect the analysis.

We now have sufficient information on what to correlate to obtain pressure drop, density and film thickness in the absence of gas viscosity. A way of determining the effects of gas viscosity is to assume a reasonable flow pattern for the gas and see how it affects the various parameters. In essence, this is a perturbation from the zero gas viscosity model.

A model which we can choose for the gas flow is that it flows as a fully developed laminar flow. This causes a problem at the bubble ends but that is ignored. If we further assume that the gas liquid interface has no slip, that is gas and liquid travel at one velocity at the interface, and the liquid in the film is traveling in fully developed laminar flow also, we have a tractable flow model. That is, we have a fully developed,viscous, annular flow. An analysis under these assumptions is performed in detail in Appendix B. The result of this analysis is a relationship between film thickness, viscosity ratio and the local gas and liquid flow rates. This relationship is combined with continuity relationships in Appendix C to obtain:

$$\frac{U_S}{U_B} = (1 - m)\left[1 + \frac{16}{\frac{(1 - m)}{m}\left(1 + \frac{\mu_\ell}{\mu_g}\frac{(1 - m)}{m}\right)}\right] \tag{34}$$

This should be a first order approximation to the film thickness around a bubble. Notice that when (μ_ℓ/μ_g) gets very large, equation (34) becomes identical with equation (31). Equation (34) is plotted on Fig. C2 with (1 - m) plotted versus (U_S/U_B) using (μ_ℓ/μ_g) as a parameter. It can be seen that for values of $(\mu_\ell/\mu_g) < 25$ the difference between (U_S/U_B) and (1 - m) as determined by equation (31) may become significant when $(U_S/U_B) < 0.80$.

This flow model also allows us to make an approximation for the pressure drop within a bubble. The pressure drop with this flow model is the laminar flow pressure drop in the gas or liquid. They are the same as is shown in Appendix B. This pressure drop can be calculated roughly from the equation:

$$\Delta P_B = \frac{8 U_B L_B \mu_g}{r_B^2} \tag{35}$$

The small velocity of the liquid is ignored in this approximation although the film thickness is accounted for. This pressure drop is not intended to be an accurate one but it should give the correct order of magnitude of any bubble pressure drop.

The effects of gas viscosity as given in equations (34) and (35) are small but can be troublesome. They are sufficiently large to cause some doubt whether to correlate (1 - m) or (U_S/U_B) while ignoring (μ_ℓ/μ_g). This must be done both ways to determine which is better, if indeed either will work. The bubble pressure drop is to be subtracted from the total pressure drop before correlation. This should be permissible provided that it is a small fraction of the pressure drop.

2.9. Gravitational Effects

In Sects. 2.3 through 2.8 of this chapter it was assumed that the flow is free of gravitational effects provided that the parameter Ω is small. Obviously, this must be an oversimplified way to neglect gravity. In this section the effects of gravity are studied with no gas viscosity. To begin with, we specify a system with the parameters:

$$N_{Re} = \frac{\rho_\ell U_B r_o}{\mu_\ell} \tag{36}$$

$$\Omega = \frac{\rho_\ell g r_o^2}{\sigma} \tag{37}$$

$$\lambda = \frac{\mu_\ell^2}{\rho_\ell \sigma r_o} \tag{38}$$

$$\frac{L_B}{r_o} \tag{39}$$

$$\frac{L_S}{r_o} \tag{40}$$

The system is the same as the system described in Sec. 2.1 of this chapter. The five parameters are equivalent to the parameters derived in Sec. 2.2. The only difference is that Ω is substituted for N_{Fr}. Also, it is assumed that Ω

is small. We now use the same technique as that used to study the effects of gas viscosity. We assume that Ω is truly zero and the flow is free of gravity. The flow is symmetric about the axis of the tube. This allows us to use all the concepts derived in Secs. 2.3, 2.4, 2.5, 2.6, and 2.7.

Let us now increase the force of gravity to the point where it no longer allows a perfectly symmetrical flow. There are two things which are likely to happen. One is that the shape of the bubble loses its symmetry. The second is that the bubble rises to the top in some way.

When these things happen the film thickness no longer is governed by the thickness at the nose. However, there should still be very little axial flow in the film. Thus equation (31) should still be valid, since m is the fraction of the cross-sectional area of the tube covered with liquid.

The value of (U_S/U_B) or $(1 - m)$ should become a function of Ω as well as λ, N_{Re}, and possibly $(\forall_S/\pi r_o^3)$. The parameters, U_S/U_B or $(1 - m)$, should still be determined at the nose of the bubbles, Thus one check of gravitational effects is to see if (U_S/U_B) or $(1 - m)$ changes with Ω, all other parameters being constant. This gives an indication whether the bubble shape at the nose is being affected by gravity.

Behind the nose of the bubble the liquid film may drain or the bubble rise, whichever viewpoint is convenient. If we ignore the axial surface tension forces we can look at the drainage as a two-dimensional, unsteady flow problem. Since the liquid film is very thin in general and should flow slowly, we assume that it flows non-inertially. That is, viscosity is the primary force preventing drainage. The Navier-Stokes equations with no inertial terms should then govern the flow in the film. The boundary condition at the wall is zero velocity and the boundary condition at the gas interface is zero shear stress. Under these conditions, the magnitude of the forces tending to distort the shape of the bubble from a circular shape is governed by the gravitational forces. Thus if Ω is small, though not zero, the bubble in two dimensions should tend to stay a circle. The rise time of a two-dimensional bubble from the center of the tube to the top can then be calculated. This calculation is carried out in detail in Appendix A. The calculation of the true rise time is tedious because it must be done numerically. A good approximation is achieved for the rise time by assuming that the bubble rises at the velocity it has when it is concentric with the tube. The time avail-

able for a bubble to rise is the time it takes for a bubble to pass a point in the tube. The analysis combines the parameters governing the rise velocity with the time available for bubble rise to give a parameter τ which can be used to determine the extent of bubble rise.

$$\tau = \frac{L_B \rho_\ell \, g r_o}{U_B \, \mu_\ell} \tag{41}$$

This parameter plus the concentricity of the bubble at the nose and (1 - m) completely determine the amount of bubble rise.

Assuming a bubble which is concentric at the nose, the value of τ at which the bubble tail will touch the top of the tube is plotted as a function of (1 - m) on Fig. A3. This value of τ is calculated from the assumption that the rise velocity is the velocity at which the bubble initially begins to rise as indicated above.

The manner in which this drainage effects the flow in the slugs is uncertain, but general statements may be made. It should make the flow there non-symmetric also. Once again this may show up in a change in (U_S/U_B). Another way this may affect the flow is that it may affect the pressure drop in the slugs.

2.10. Flow Regime

Any flow in a horizontal tube which fits the description given in the introduction should properly be called a horizontal capillary slug flow. This would be of little value to us, however, because the only flow which is studied here is a horizontal capillary slug flow with certain restrictions. These restrictions are therefore included as part of the specifications for the horizontal capillary slug flow. Initially these restrictions are made as:

1. $\rho_\ell/\rho_g \gg 1$
2. $\mu_\ell/\mu_g \quad 1$
3. Ω is very small.

The results of the experiments combined with the analyses should yield a better limit for (μ_ℓ/μ_g). The limit for (ρ_ℓ/ρ_g) has not been discussed, but because of

the very, very large ratio for most liquids and gases, it is felt that any lower limit is exceeded in most cases. The third requirement has only been postulated. The effects of variation in Ω must be studied experimentally and its results included in the flow regime specifications.

The discussion above has been concerned with the problem of whether a given long bubble flow is one which has been studied here. There is another possibility and that is that the above specifications may be met but the flow may still not be a long bubble flow. The existence or non-existence of a long bubble flow in this case must be determined by the four parameters of Sec. 2.3, N_{Re}, λ, (L_B/r_o) and (L_S/r_o), or an equivalent set. The exact determination of flow regime changes is closely linked to the results of the experiments, so further discussion of flow regime boundaries is halted until the results of the experiment are discussed.

2.11. Results of Analysis

The analytical results of this chapter show that if gravity and gas viscosity may be ignored, the pressure drop, density and film thickness may be correlated as a function of N_{Re}, λ and $(\mathcal{V}_S/\pi r_o^3)$. They can be correlated using measurements of pressure drop per bubble and slug, slug velocity, bubble velocity and $(\mathcal{V}_S/\pi r_o^3)$.

The effects of viscosity and gravity can be approximated with simple analyses. The results of these analyses can be used to check the reasonability of the assumption of no gravitational forces or gas viscosity. The effect of gas viscosity on film thickness is checked by equation (34). The effect of gas viscosity on pressure drop is calculated from equation (35). The gas viscosity does not affect density except that it may affect (U_S/U_B). The gravitational forces are checked by observing the effect of Ω on (U_S/U_B) or $(1 - m)$ and pressure drop. Also the bubble rise analysis checks film thickness changes due to gravity.

Unfortunately, the two effects, gas viscosity and gravity, cannot be separated well in a practical experiment. It was hoped that the experimental results would show some means of separation.

3. EXPERIMENTAL TECHNIQUES AND MEASUREMENTS

3.1. Required Measurements and Methods of Measurement

The analyses of Chapter 2 show what measurements are required to correlate pressure drop, density and film thickness in the absence of a gravity field and gas viscosity. They are the pressure drop per bubble and slug, bubble velocity, slug velocity and $(\mathcal{V}_S/\pi r_o^2)$. In addition to these measurements the bubble length is also required to check the effect of gas viscosity on pressure drop and the effect of gravity on bubble rise.

The measurements are made on a system similar to the model for analysis. This is, of course, the only way where a single value of $(\mathcal{V}_S/\pi r_o^3)$ and (L_B/r_o) has any meaning.

The pressure drop is measured over a large number of bubbles over a given length of tube. The bubble length and the bubble and slug length are measured. Thus the number of bubbles and slugs in a test section are known, and the pressure drop per bubble and slug can be found directly.

The bubble velocity is found from this same measurement of bubble and slug length and a measurement of bubble frequency. The slug velocity is found from measurement of the gas and liquid flow rates and the use of equation (17).

The equipment to make these measurements and the whole experimental test system are explained in the next section.

3.2. Experimental Apparatus

An apparatus was constructed to create a uniform bubble and slug flow and to measure the various parameters. A schematic outline of the apparatus is shown in Fig. 5. It is a once through system designed to make all measurements simultaneously.

The liquid reservoir is a pressurized container (a pressure cooker) which holds a polyethylene container of liquid. The reservoir is pressurized by the same gas supply which is used to supply gas to the test section. The connections are sufficiently interchangeable so that the liquid can be saturated with gas before a test run. The liquid goes from the reservoir to the bubbler.

The bubbler is a device to bring the gas and liquid together in such a way that uniform bubbles and slugs are formed. It consists of a conical section of

plexiglas, through which the liquid is introduced, and a piece of stainless steel hypodermic tubing, through which the gas is introduced. The conical section tapers gradually from around a half inch diameter to the diameter of the test section or slightly larger. The hypodermic tubing is placed along the axis of the conical section and can be moved along the axis. The tubing is approximately one sixteenth of an inch in diameter. The bubble and slug lengths may be varied by varying the position of the hypodermic tubing and its size. The gas and liquid flow rates are regulated with needle valves located as close as possible to the bubbler. This is essential to obtaining a well regulated flow. The bubbler was tried in both a vertical and horizontal position. It worked both ways but it was found that at higher velocities there was great difficulty in turning the bubbles back to the horizontal direction. Therefore, the horizontal position was judged to be the best all around position, although some data was taken with a vertical orientation at low velocities.

From the bubbler the two phases flow through a calming section of at least 500 diameters in length. This serves to both saturate the liquid and gas with gas and liquid respectively and to eliminate entrance effects on the test section. The flow goes from the calming section directly into the test section. The test section may be the same tube as the calming section or it may be another piece of tubing of about the same diameter which is connected to the calming section with a special fitting. The division of the test section from the calming section is a pressure tap. The pressure tap may go right into the tubing or may go into the special fitting. This special fitting is a piece of plexiglas with a hole in it of the test section diameter. The fitting allows both the calming section and the test section to be lined up with it so that the flow sees little change in diameter.

The tubing for the test section and the calming section is precision bore borosilicate glass tubing with a diameter tolerance of $\pm$ 0.0003 inches. The tubing in the test section was calibrated by measuring liquid flow rate through it and measuring pressure drop. This gives an over-all average radius of the tubing. In all but two of the cases, the test section diameters fell within the tolerances when calibrated this way. The two cases where they did not were not sufficiently far off to cause any problems. The calibrated radii were used in calculations.

From the test section the flow goes to a gas liquid separator. From the separator the gas and liquid go to separate metering systems. Both metering systems are capillary tubing laminar flow meters.

Four gas metering tubes are connected through a manifold to the gas liquid separator. They are ordinary capillary tubing of the order of one half to one millimeter in diameter and one meter in length. The different tube sizes and possible combinations of tubes allow a considerable range of flows. The pressure drop for the tubes is measured with a manometer also connected to the manifold. The connecting tubes and the manifold are of sufficient diameter so that very little pressure drop occurs in them. The tubes are sufficiently long and the velocities sufficiently low so that entrance effects in the tubes are negligible. The maximum pressure drop allowed through the tubes is about 20 centimeters of water. This keeps the compressible effects small. For isothermal flow in the tubes the compressibility is less than two per cent with a pressure drop of 20 centimeters of water. This small amount of compressibility, however, is accounted for by taking the measured flow rate to be the volume flow rate at the average pressure of the tube entrance and exit (atmospheric). The temperature of the gas is taken to be the temperature of the liquid. This is usually within one degree Centrigrade of ambient temperature in the experiments, so it should be valid.

The tubes were calibrated with air saturated with water vapor. The viscosity of the saturated air was calculated from the formula of Wilke[18] for a binary mixture. This formula gives a viscosity for saturated air of about two per cent less than the viscosity of dry air. Then, since the formula should give only an approximate answer, the calibration was checked with water in two tubes. This showed that the viscosity as determined by the formula of Wilke gives about the same calibration for the tubes as does water. The calibrations with air saturated with water were then accepted as true. Then each possible combination of liquid vapor and gas was checked in the tubes. The viscosity of each mixture was determined at saturation conditions. It was found that mixtures of nitrogen and heavy hydrocarbon vapors (heptane, octane) have a much greater decrease in viscosity than air does with water. The order of magnitude is properly predicted by the formula of Wilke, but for flow measurement purposes, it was considered necessary to measure the viscosity of the mixtures at each temperature where it was used.

This technique of measuring viscosity by measuring the flow rate and pressure drop should give a value of viscosity which, when used in the reverse procedure (from pressure drop and viscosity calculate flow rate), should give a result as accurate as the initial flow rate measuring method. The original flow measuring method, or the calibration technique, should be accurate to about two per cent.

This measured gas flow rate is unfortunately not necessarily the value of Q_g in the test section. A small but finite amount of compressibility must be taken into account in the test section. This is done by assuming that the average gas flow rate in the test section is the flow rate if the gas were at a pressure which is the average of the inlet and outlet pressure. Assuming that this is isothermal flow, we can say:

$$\frac{v_2}{v_1} = \frac{p_1}{p_2} \tag{42}$$

where 1 represents conditions at the average pressure (as determined above) in the test section and 2 represents conditions at the average pressure in the meter tube.. Now the ratio (v_2/v_1) should also be equal to the ratio of gas volume flow rates, (Q_{g2}/Q_{g1}). Therefore, we can write:

$$\frac{Q_{g2}}{Q_{g1}} = \frac{p_1}{p_2} \tag{43}$$

Q_{g2} is measured and so are p_1 and p_2. Therefore, we can calculate Q_{g1}. In this case only Q_{g1} and Q_{g2} are not the instantaneous flow rates as given elsewhere, but are the average flow rates at 1 and 2.

Some objection might be raised at this point because all analyses were made for incompressible flow. The only defense for the actions here is that some compressible effects are inevitable. In this case, they never go over twenty per cent. The corrections, therefore, are never more than ten per cent. In a case where the effects are this large, too large to ignore but still not excessive, an averaging procedure for the flow rate appears to be a reasonable way to handle it. It is known that somewhere in the tube, the results obtained are true.

The liquid flow goes from the separator, past a thermometer then to a manifold. From the manifold the liquid can be made to flow in one, two, or three tubes. Each of these tubes is of a different size in diameter and length. These tubes each have a manometer system to measure pressure drop across them. Entrance effects are made negligible in these tubes by having long calming sections or low flow velocities. Care is always taken to assure laminar flow in these tubes.

As in the case of gas tubes, these tubes were calibrated for each liquid. These calibrations showed that the viscosities and densities of the liquids tested were not quite those reported in the literature. The differences were considered big enough to take into account for flow measuring purposes but not enough for other uses.

The accuracy of the liquid metering system is not as great as that for the gas metering system. The reason for this is that the liquid viscosities in general are much more sensitive to temperature than are gas viscosities. The worst offender is water. At 25°C its viscosity changes 2.5 per cent per degree C. The liquid temperature is measured just ahead of the manifold to $\pm$ 0.1°C with a thermometer. The ambient temperature is measured to this accuracy also. As long as there is a difference between liquid and ambient temperature not much greater than 1°C, there should be an error due to temperature of less than 2.5 per cent. This is true in most cases in the experiments and the worst case is where the difference is about 1.5°C. In addition to this error, there is still the possible error in calibration flow measurement of about one per cent. Thus the total error can be in the order of three or four per cent.

These two flow meters were used in most of the experiments. In some of the early experiments, the flow was collected and timed. The gas was collected by displacement of liquid in a volumetric burette and the liquid was collected in a graduated cylinder. Also in some of the low liquid flow rate experiments the liquid was collected and timed while the gas was metered through the gas tubes. These techniques of measuring the flow give as good or better answers than the flow meter tubes, for they are the same techniques used to calibrate the meter tubes.

The pressure at the entrance to the test section is measured by a manometer leading from the tube at that point. For low pressure drop only one leg of the manometer is used. For high pressure drops three legs are used. The second two legs are separated from the first leg with a column of air. The first leg is, of course, always filled with the test fluid. The second and third legs are filled with that or some other suitable fluid. The pressure at the end of the test section is obtained from the manometer on the separator. It is the same manometer used to measure pressure drop for gas flow.

The bubble and slug lengths are measured with a Polaroid camera and a strobe light. The flow is photographed and the bubble and slug lengths are measured from a meter stick which is located next to the test section. Sample photographs of slug flow are shown in Fig. 6. By measuring the over-all length of a number of bubbles and slugs, one can obtain a fairly accurate (about $\pm$ 2 per cent) value of the average bubble plus slug length. The bubble frequency is measured with a strobotac.

The camera also allows a good visual study and record of the flow regime. It shows the type of flow quite well.

3.3. Experimental Procedure

A standard procedure was adopted for taking experimental data. Small deviations were occasionally made from this procedure but no great deviations were found in the results.

The liquid reservoir is saturated with the gas by bubbling gas into the reservoir through the liquid outlet line. This is done at atmospheric pressure. After the liquid is saturated with gas, the connections are switched to that shown on Fig. 5. Care is taken to assure that the gas pressurizing the reservoir remains essentially pure while switching connections.

The reservoir is then pressurized to some pressure between two and ten psig. The liquid valve on the bubbler is then opened and all the liquid meter tubes and manometers are filled. The liquid meter tubes are then closed off. All valves on the gas metering system are closed also at this time and the test section manometer is filled with liquid to a level above the expected pressure drop. The test section manometer is then closed off. A preselected bubble and slug length and bubble frequency are set to flow through the bubbler, and the

proper meter tubes are opened. When equilibrium is reached in flow rates, bubble and slug length, and bubble frequency, the test section manometer is opened. The overcharging of the manometer assures that no gas flows into the manometer. When this manometer comes to equilibrium, all the data is taken.

4. EXPERIMENTAL RESULTS

4.1. Discussion of Experiments

The experiments described in Chapter 3 were run with various sized tubes and various liquids and gases. The experiments were run at ambient temperature which ranged from 20°C to 30°C. The bulk of the experiments were run at close to 25°C. A brief summary of the various combinations of liquids and gases used is given below in Table A. Normal heptane and normal octane were used in the experiments. References to heptane and octane in the text refer to these fluids.

TABLE A

Number	Liquid	Gas	Tube Radius (nominal)
1	Water	Air	0.0514 cm
2	Water	Nitrogen	0.0514 cm
3	Water	Air	0.0795 cm
4	Water	Nitrogen	0.0795 cm
5	N-Heptane	Nitrogen	0.0514 cm
6	N-Heptane	Nitrogen	0.0795 cm
7	N-Heptane	Helium	0.0514 cm
8	N-Octane	Nitrogen	0.0514 cm

The bulk of the data was taken with the first six of the possible combinations. The reason for this is that heptane and water have the same value of λ for a given radius tube. This is in spite of the fact that ρ_ℓ, μ_ℓ and σ are each different in the two liquids. This made the data plotting much simpler. For a given sized tube the data for the two liquids could be plotted versus N_{Re} with only one parameter, $(\mathcal{V}_S/\pi r_o^3)$.

By using two different sized tubes, λ was varied to a certain extent. After the correlations were well established the last two systems were tested. Helium was tested with heptane to test the effect of gas density on one flow regime boundary. The octane-nitrogen system was tested to show the effect of varying λ further.

These systems had different values of (μ_ℓ/μ_g) and Ω. The value of (μ_ℓ/μ_g) was varied between approximately 25 and 50. The value of Ω was kept small enough so that with zero velocity the bubbles were distorted very little. For this to occur, Ω must be small compared to one. Ω was kept smaller than 0.22.

The results of the experiments are first discussed under the assumption that (μ_ℓ/μ_g) and Ω do not affect the flow. After that the effects of (μ_ℓ/μ_g) and Ω are discussed.

4.2. Pressure Drop

The analysis of Chapter 2 states that at low N_{re} we should be able to state the pressure drop per bubble and slug as:

$$\frac{\Delta P}{\frac{\mu_\ell U_B}{r_o}} = \frac{8\,\mathcal{V}_S}{\pi r_o^3} + K \qquad (44)$$

where K represents some end effects. These end effects may be functions of λ and N_{Re}, but not of $(\mathcal{V}_S/\pi r_o^3)$. Initially, the data for different values of λ were plotted on separate graphs with the coordinates $(\Delta P/\mu_\ell U_B/r_o)$ and $(\mathcal{V}_S/\pi r_o^3)$. N_{Re} was indicated as a parameter on these plots. It was found that at $0<N_{Re}<270$ the plots for the different values of λ fell on the same straight line. Thus the data were all plotted on one graph. This is shown on Fig. 7. The values of λ and the other experimental conditions for Fig. 7 as well as the rest of the data are shown in Appendix D. A line with a slope equal to 8 and intersecting the $(\Delta P/\mu_\ell U_B/r_o)$ axis at 45 fits the data quite well. This means that the equation (44) is reasonably valid and the end effect is a constant. Equation (44) can then be written:

$$\frac{\Delta P}{\frac{\mu_\ell U_B}{r_o}} = \frac{8\mathcal{V}_S}{\pi r_o^3} + 45 \qquad (45)$$

This equation is valid in the range of N_{Re}, $0<N_{Re}<270$. This range of N_{Re} is called Region I.

It appeared that for a certain range of $N_{Re}>270$ the form of equation (44) should still be valid. The end effect term would have to be changed, of course.

The end effect was experimentally determined using the different values of λ as before and varying N_{Re}. This value of K was plotted on separate graphs for each value of λ as a function of N_{Re}. Once again, these plots showed no dependence on λ. The data showed that K could be approximated as:

$$K = 0.163 \quad \frac{\rho_\ell U_B r_o}{\mu_\ell} \tag{46}$$

for a range of N_{Re}, $270 < N_{Re} < 630$. This range of N_{Re} is called Region II. In Region II the equation (44) takes the form:

$$\frac{\Delta P}{\frac{\mu_\ell U_B}{r_o}} = \frac{8 \mathcal{V}_S}{\pi r_o^3} + 0.163 \quad \frac{\rho_\ell U_B r_o}{\mu_\ell} \tag{47}$$

By multiplying both sides of equation (47) by $(\mu_\ell U_B / r_o)$, one would see that the end effect term is an inertial pressure drop. The data showing the validity of equation (47) is shown on Figs. 8, 9, and 10. As can be seen on these figures, equation (47) is reasonably valid.

At a value of N_{Re} of 630 the value of K as a function of N_{Re} suddenly drops and then rises again gradually. The data begins to spread as a function of $(\mathcal{V}_S / \pi r_o^3)$. Thus the value of K becomes a function of $(\mathcal{V}_S / \pi r_o^3)$, and its basic meaning is destroyed or at least as a tool it becomes of little worth. Therefore, the range of $N_{Re} > 630$ must be correlated by more complex means. This range of N_{Re} is called Region III. It was expected that since λ did not affect the pressure drop correlations in the lower N_{Re} regions, it would not affect pressure drop in Region III. Thus $(\Delta P / \mu_\ell U_B / r_o)$ was plotted as a function of N_{Re} with $(\mathcal{V}_S / \pi r_o^3)$ as a parameter. The data and all the experimental conditions for Region III are shown plotted on Fig. 11. It can be seen by inspection that the data does appear independent of λ in Region III also. As before, a simple equation can be written for the pressure drop in this region. It is:

$$\frac{\Delta P}{\frac{\mu_\ell U_B}{r_o}} = 80 + \left(0.02 + 0.011 \quad \frac{\mathcal{V}_S}{\pi r_o^3} \right) \quad \frac{\rho_\ell U_B r_o}{\mu_\ell} \tag{48}$$

However, this equation cannot be as well explained physically as equations (45) and (47) were explained in Chapter 2. For this reason, it appears that it should not be used outside the range of variables tested. The correlations may change in character completely outside the tested range whereas it is reasonable that in Regions I and II the correlations should be valid outside the range of test variables.

Region III does not necessarily extend to infinite N_{Re}. There is a very definite boundary on N_{Re}. As velocities go up, the tails of the bubbles begin to break up into small bubbles. This is a flow regime transition. Generally, in the experiments here all the transitions occurred at a value of N_{Re} of around 2000.

This is not the criterion of transition, but it explains why all the data cuts off at around that N_{Re}. The data shown is all in slug flow.

The correlations for pressure drop are all obtained from data for pure liquid systems. That is, the liquids in the systems are pure compounds. It was found that systems which are not pure have entirely different results for pressure drop.

The question of importance is what is a pure compound. A pure compound is defined here as one which has the viscosity, density and surface tension of a pure compound as reported in the literature. Of these the greatest importance is the surface tension. It is the property most easily disturbed by impurities, and of common liquids water is the liquid most easily disturbed.

It was found that when new Tygon tubing (cleaned with detergent and rinsed) was used in the liquid inlet lines, the surface tension of the water decreased by about nine per cent. This decrease affected the pressure drop quite strongly as can be seen in Fig. 12 for data taken in Region I.

This result is surprising since everywhere else the pressure drop is independent of surface tension (as shown by independence from λ). It is attributed to the nature of surface tension when it is decreased by a small amount of contaminant. When water is contaminated with small amounts of alcohol, it is known that the surface tension is a function of the time which a surface has existed. It is likely that this contaminant, though its exact nature was not investigated, is of the same nature. If this is so, the surface near the nose of

a bubble essentially sees a higher surface tension than the surface at the tail. This would cause shear stresses in the liquid film and some pressure drop.

Because of the infinite number of possible contaminants and degrees of contamination this problem was investigated no further. Care was taken after this phenomenon became known to measure a sufficient number of surface tensions to insure pure liquids.

The effect of gas viscosity on the pressure drop was corrected for by using equation (35). This equation accounts for gas viscosity and bubble length in one step. The corrections were made only on Figs. 7 through 11. The corrections were of such a small nature that it was not felt to be worthwhile to make them on Fig. 12. The results of that figure would not be changed by such a correction. Further discussions and justification of this correction are given in Sec. 4.4 of this chapter.

Bubble lengths varied quite strongly in the data for Regions I and II. Little systematic work was performed in varying bubble length but a random distribution did occur. As the data shows, no differences were found due to bubble length once the minor effects of gas viscosity had been accounted for.

4.3. Velocity Ratio

The velocity ratio (U_S/U_B) should be a function of N_{Re}, λ, and possibly $(\mathcal{V}_S/\pi r_o^3)$ according to the analysis of Chapter 2. It turns out, however, that a different parameter is more suitable for plotting velocity ratio. This parameter is obtained by combining N_{Re} and λ. It is:

$$\Psi = \frac{\mu_\ell U_B}{\sigma} \tag{49}$$

There is no loss of generality in plotting data as a function of Ψ and λ as opposed to N_{Re} and λ.

The systems with λ equal to approximately 2.1×10^{-5}, which include water-air, water-nitrogen, heptane-nitrogen, and heptane-helium in a tube of 0.0514 centimeters nominal radius, have their velocity ratio data plotted on Fig. 13. The plot is of (U_S/U_B) versus Ψ. The value of $(\mathcal{V}_S/\pi r_o^3)$ should be a parameter on this plot, but the data all appear to fall on one line without

inclusion of this parameter. The scatter which is present can be explained as experimental scatter for the most part. In one region, however, the scatter does appear to be systematic with $(\mathcal{V}_S/\pi r_o^3)$. That is the area where the data breaks away from a straight line at $\Psi = 19 \times 10^{-3}$ to the point where it reaches a constant value at $\Psi = 51 \times 10^{-3}$. In this region the data have a systematic increase in (U_S/U_B) with decreasing $(\mathcal{V}_S/\pi r_o^3)$. The differences are not so large that the exact nature of the variation can be determined. In fact, the data appear to have little greater spread than the random scatter at higher and lower Ψ. Since the spread is so small, it is not considered of great importance, and the data in the region of systematic variation is approximated with one line as it is elsewhere.

The data with λ equal to approximately 1.5×10^{-5}, which again include water-air, water-nitrogen and heptane-nitrogen systems, but in a larger diameter tube, are shown in Fig. 14. The same arguments apply to Fig. 14 as applied to Fig. 13 except that the region where (U_S/U_B) is systematically dependent on $(\mathcal{V}_S/\pi r_o^3)$ is shifted to the left.

The data for an octane-nitrogen system with λ equal to approximately 3.4×10^{-5} in a tube of 0.0514 centimeter radius is shown on Fig. 15. As can be seen, this data takes the same general shape as the data on Figs. 13 and 14. The region where there is a systematic variation with $(\mathcal{V}_S/\pi r_o^3)$ is also present.

The best fit lines of the data of Figs. 13, 14, and 15 are shown together on Fig. 16. In addition, the empirical relation for (U_S/U_B) obtained by Fairbrother and Stubbs[6] is shown. Their relation, though not stated in these terms, corresponds to a very high value of λ. Thus we have a limiting value of all the curves. Another plot, taken from Fig. 16, is shown on Fig. 17. It is a somewhat more useful relation at times. It is a plot of (U_S/U_B) versus $(\mu_\ell U_S/\sigma)$.

At low Ψ all the curves except the high λ curve appear linear with Ψ. This region corresponds roughly to Regions I and II of the pressure drop correlations. There is then a general breaking away from the linear relations, and eventually the curves achieve a minimum and return to approximately 0.84. It should be of interest to point out that though some of the data shown on Figs. 13, 14, and 15 are in the bubbly slug flow regime as described in the pressure drop section, the value of (U_S/U_B) remains at the constant value.

The most pertinent questions about the behavior of these curves are why do they go through a minimum, and why do they approach a constant value. The latter question is discussed first, and from that a possible explanation of the former is given.

Nicklin et al[17] found similar results when working with slug flow in larger vertical tubes. They found that they could write the equation for bubble velocity as:

$$U_B = \Gamma U_S + 0.35\sqrt{2gr_o} \tag{50}$$

where Γ is a constant equal to 1.2 when the Reynolds Number based on liquid properties, U_S and pipe diameter is greater than 8,000. The second term on the right is the Taylor bubble rise velocity. That is the velocity which a bubble draining a tube of liquid covered at the top would attain if the liquid were in potential flow.

Nicklin and his associates explained the value of Γ equal to 1.2 very simply. Their explanation is that the bubble travels at the Taylor bubble rise velocity plus the velocity that the bubble sees at the nose of the bubble. U_S is the average velocity in a slug, but the velocity at the centerline in a turbulent profile is approximately $1.2\ U_S$. There the bubble nose would see a velocity of $1.2\ U_S$.

In the absence of a gravity field this explanation would say that the bubble would travel at slug centerline velocity or:

$$\frac{U_S}{U_B} = \frac{1}{1.2} = 0.83 \tag{51}$$

In the case of a horizontal capillary tube, there should be no gravity effects on the bubble velocity. If the explanation that the bubbles then try to flow at slug centerline velocity is true, then the velocity ratio should be as in equation (51), provided that the slugs are in turbulent flow.

The values of N_{Re} at which (U_S/U_B) becomes a constant is not the same for all the curves. They are, however, always greater than 1700. This corresponds to a Reynolds Number as defined by Nicklin of about 2900. This Reynolds Number is rather borderline to say that the slug is in turbulent flow, but it is quite possible that it is. The constant value of (U_S/U_B) of 0.84 compares favorably with Nicklin. These facts indicate that it is quite likely that the bubbles are traveling at centerline velocity and the slug is in turbulent flow. This is especially so since at greatly increased Ψ where the Reynolds Number is large enough to insure turbulent flow, the value of (U_S/U_B) is still around 0.84 in all the data.

The tendency of the bubble to travel at slug centerline velocity might be expected to explain the total behavior of the (U_S/U_B) curves. At low velocities the slug is in laminar flow so the slug centerline velocity is twice the average slug velocity. If the argument in turbulent flow were valid in laminar flow, the value of (U_S/U_B) would then be 0.5 for low velocities. This is not so by experiment; therefore, there must be more to the explanation. Bretherton[4] found that he could predict the value of (U_S/U_B) at very low values of Ψ by considering only the flow in the region where the film tapers to a constant thickness. Only viscous and surface tension forces were considered in his argument. His solution is not too dissimilar from the empirical Fairbrother-Stubbs relation. From his results one might argue that the viscous and surface tension forces tend to decrease (U_S/U_B) with increasing velocity and that they tend to act near the film. One can hypothesize that (U_S/U_B) is controlled by these forces near the film at low velocities and is controlled by the inertial forces near the centerline at high velocities. This would explain the shape of the curves. As velocity is increased inertial forces tend to cause (U_S/U_B) to break away from a curve where it is controlled by viscous forces. Eventually the inertial forces get large enough to cause (U_S/U_B) to be controlled entirely by the centerline velocity. This is where (U_S/U_B) achieves a value of 0.84.

The shapes of the curves indicate that one can interpolate for intermediate values of λ. The limiting case for λ very large can be considered as the Fairbrother-Stubbs curve. As λ increases beyond 3.4×10^{-5}, the curves will get more and more like the very large λ curve but should still break away and return to 0.84. As λ increases the minimum point for (U_S/U_B) should occur at higher values of Ψ. This interpretation is gained from the general shape of

the experimental curves and from the explanation for the shape of the curves. On the other extreme, as λ approaches zero, it would appear that the (U_S/U_B) curve does not necessarily go to a minimum but simply comes down to a value of 0.84. A limit might be that (U_S/U_B) is everywhere equal to 0.84.

4.4. Effects of Gas Viscosity and Gravity

One effect of gas viscosity has already been mentioned in the pressure drop discussion. The data for pressure drop have incorporated in them a correction for gas viscosity. This correction subtracts out the pressure drop within a bubble. The correction is based on equation (35) for a cylindrical bubble with a laminar flow velocity profile. This correction should be reasonably valid when the viscosity ratio is large and the film thin so that the film velocity is low and the bubble is somewhat symmetrical. Further, it should only be used as a small correction term for the pressure drop over one bubble and slug. The minimum value of (μ_ℓ/μ_g) of about 25 and the minimum value of (U_S/U_B) of about 0.77 would appear to meet the requirements for viscosity ratio and film thickness. Equation (35) gives corrections of the order of less than five per cent of the total pressure drop, which should satisfy the requirement for a small correction. It is concluded that this correction should correctly take care of the pressure drop in a bubble and eliminate any consideration of it in correlating pressure drop.

The other effects of gravity and gas viscosity on the data for pressure drop and velocity ratio can be studied with the use of three parameters, (μ_ℓ/μ_g), Ω, and τ. Only the first two should be required to study velocity ratio, but all three are required for pressure drop. These effects are best studied from the data of Figs. 13 and 14.

On each of these figures, λ is a constant, but the values of Ω and (μ_ℓ/μ_g) are not, however. The data on each figure fall on one line regardless of whether (μ_ℓ/μ_g) and Ω are different. It appears that (U_S/U_B) is free of gas viscosity and gravitational effects for this data. It is possible, of course, that the effects of (μ_ℓ/μ_g) just cancel the effects of Ω, but this appears unlikely for two curves over large values of Ψ.

The freedom from gravitational effects indicates that the bubbles are centered, at least at the nose of a bubble. Behind the nose of a bubble the liquid drains as a function of τ. The values of τ for the data of Figs. 13 and

14 ranged from a value where it would be expected that a bubble is still symmetric at the tail to a value where more than twice enough time for a bubble to rise to the top had been allowed. This effect would not be expected to be noticed in the velocity ratio because that should be determined near the nose, even with the possible side effects of gravity and gas viscosity. It may show up in the pressure drop, however. As was seen in the pressure drop discussion, all of the pressure drop data, some of which was taken simultaneously with the data corresponding to that on Figs. 13 and 14, is well correlated without consideration of τ. The values of Ω, (μ_ℓ/μ_g), and even λ are not required for that either. It is concluded that other than the minor correction for bubble pressure drop, all the pressure drop data is independent of gravity and gas viscosity.

The symmetry of the bubble near the nose should also mean that the film thickness near the nose can be calculated from equations (C5) and (32). The independence of (U_S/U_B) from gas viscosity means that film thickness calculated from equations (C5) and (32) is not free of gas viscosity. The difference between (U_S/U_B) and $(1 - m)$ is as high as about 10 per cent for the data of Figs. 13 and 14. The lack of symmetry which may exist near the tail of the bubble prohibits the calculation of film thickness there. Nevertheless, the value of $(1 - m)$ should not have been much different near the tail because the gas viscosity should not have caused much flow in the liquid film.

Until now it has been shown that all the pressure drop data and the velocity ratio data for Figs. 13 and 14 are free of gravitational and gas viscosity effects. In addition, the noses of the bubbles in the data for Figs. 13 and 14 are probably symmetrical whereas the tails may not be. The next set of data to be discussed is the data for Fig. 15.

The data for Fig. 15 can also be argued to be free of gravitational and gas viscosity effects. First of all, the pressure drop data for it correlates with the other pressure drops where gravitational and gas viscosity effects were ignored. Secondly, Ω is equal to 0.085, which is less than the value of Ω for some of the data of Figs. 13 and 14. Lastly, the curve of (U_S/U_B) appears to be a reasonable interpolation between the curves for $\lambda = 2.1 \times 10^{-5}$ from Fig. 14 and λ very large. The λ very large curve has been shown to be symmetrical by others, and is concluded to be free of gravitational effects. It should be free of gas viscosity effects also.

The conclusions are that the data plotted on Figs. 7 through 15 are free of gravitational and gas viscosity effects although some of the parameters of the flow, such as film thickness, may not be.

The above description is taken to be a description of the type of horizontal two phase slug flow studied here. Rather than the flow model analyzed in Secs. 2.1 through 2.7 of Chapter 2 which is entirely free of gravity and gas viscosity, a flow is taken for which only the pressure drop and velocity ratio are necessarily free of gravitational effects. The density, because it comes from continuity and velocity ratios, is also free of gravity and gas viscosity. The film thickness unfortunately is not. The film just behind the nose is assumed to be symmetrical because of the independence of (U_S/U_B) from gravity. Therefore, just behind the nose of the bubble the film thickness should be calculatable from equations (C5) or (31) and (32). If the value of τ is small compared to complete bubble rise time, the drainage should not be great and the film thickness near the tail should be much the same as near the nose. Otherwise the film thickness cannot be calculated because the analysis of Appendix A for the bubble rise is only valid for zero gas viscosity and gives only a criterion for the order of magnitude of the rise time. The only thing which may be calculated to some extent is $(1 - m)$. It should not be too different from the value at the nose because of the low velocities in the film in most cases.

It should be pointed out that the flow regime description includes a zero gravity field. That is, the flow need not be entirely free of gravity, but it may be.

For the data to be of value, the conditions under which the data can be applied must be specified. This is, of course, a part of the flow regime specification. Clearly, it must be possible to make Λ somewhat larger than the maximum value tested and (μ_ℓ/μ_g) somewhat smaller than the minimum values tested and still have the same results. The maximum and minimum values of Λ and (μ_ℓ/μ_g) will of course depend on the other parameters also. Since a complete parametric study would be impossible, it is assumed that the maximum value of Λ and the minimum value of (μ_ℓ/μ_g) tested here can be used as limits. Therefore, as one boundary we take $\Lambda < 0.22$ and as another, $(\mu_\ell/\mu_g) > 25$. The data was, of course, all taken for $(\rho_\ell/\rho_g) \gg 1$, and this criterion must apply also.

4.5. Flow Regime

The previous section described the geometry of a horizontal capillary slug flow in detail. The flow is assumed to be possible where:

$$\frac{\rho_\ell}{\rho_g} \gg 1 \tag{52}$$

$$\frac{\mu_\ell}{\mu_g} > 25 \tag{53}$$

$$\Omega < 0.22 \tag{54}$$

Any horizontal slug flow which meets these requirements is considered to be of the type of horizontal capillary slug flow discussed here. The characteristics of this flow are that the effects of gas viscosity and density and of gravity can be ignored for velocity ratio and pressure drop. The film thickness anywhere except near the nose of the bubble is not determined for this regime except in certain circumstances. This is because the nose of the bubble is concentric, but the rest of the bubble need not be.

When the conditions (52), (53), and (54) are met, there are still several types of flow which may exist in a tube. These are discussed next.

The experiments showed the existence of two slug flow boundaries. One is predicted by analysis with some experimentally determined parameters, and the other is determined completely empirically. The first is a transition to an annular flow. The second is a transition to a flow where the tails of the bubbles begin to break up into many small bubbles. This is called a bubbly slug flow. They are discussed in this order.

The slug flow regime should be bounded in the region of very low liquid to gas flow ratios by a transition to annular flow. This transition is the point where bubbles get so long and the slugs so short or few that the slugs carry very little liquid. To demonstrate how this transition comes about, one can look at it from two viewpoints. One can look at an annular flow and see what is required to make it into a slug flow or one can look at a slug flow and see what is required to make it into an annular flow. Since we are interested here

in the transition to an annular flow, we will take the latter viewpoint.

Consider a steady, incompressible, slug flow in a tube at some arbitrary Q_ℓ and Q_g with uniform bubble and slug lengths and no gravitational effects. By steady it is meant that U_S and U_B are constant in time. Now let the gas flow be increased and the liquid flow be decreased so that the sum of the two remain constant. That is, U_S remains constant. This causes the bubble to slug length ratio to increase. If the sum of the bubble and slug length are kept at some reasonably small value, the bubbles eventually begin to touch each other, then coalesce into longer bubbles. At the point where the slugs disappear, there should be no liquid flow other than that which occurs in the liquid film due to shear forces. This can be called the transition to annular flow.

At the transition point the film thickness is still related to a bubble velocity and a slug velocity. This relation is given by equation (C5). The gas-liquid flow ratio should be given by the equation for annular flow, equation (B14).

If (Q_g/Q_ℓ) becomes greater than the value which it has at the transition point, the film thickness will decrease as could be seen by inspection of equation (B14). It can be shown that if for any reason a slug should occur in a flow where the film is thinner than at transition, the slug would disappear after moving some distance down the tube.

Annular flow may not occur when (Q_g/Q_ℓ) is less than the value at transition. If it did, the film would have to be thicker than it is at the transition described above. If such a flow should somehow occur and a slug should somehow be formed in it, the slug would leave a film at the thickness of transition and the slug would grow in length. It has been shown by theory and experiment[12] that in an annular film such slug formation does occur. Thus an annular flow with (Q_g/Q_ℓ) less than at transition would degenerate to a slug flow.

The arguments for a boundary between slug and annular flow have been made without consideration of gravity. As might be expected from the analysis for gravitational effects, the long bubbles which become annular flow should drain considerably to form a stratified flow. This drainage is ignored in the analysis and is shown not to change (Q_g/Q_ℓ) at the boundary to a great degree in the experimental results.

The boundary is sufficiently well specified to calculate its location. As is indicated from the arguments for a transition, specification of (Q_g/Q_ℓ) and the inlet conditions to the tube might be a better way to describe the geometry of the flow than bubble and slug length. In addition to these specifications, three other parameters are required in the absence of gravity to completely specify a flow. These are taken here to be $(\mu_\ell U_S/\sigma)$, (μ_ℓ/μ_g), and λ. These five parameters should describe any flow within the limitations made on gravity. One of these appears to be unimportant for this flow boundary. That is the inlet condition. Therefore, we need specify only four parameters to specify the boundary. It is understood, of course, that from previous arguments (μ_ℓ/μ_g) should be much greater than one.

As indicated above, equations (C5) and (B14) can be used to calculate the location of the transition. They are repeated here as:

$$\frac{U_S}{U_B} = (1 - m)\left[1 + \frac{16}{\frac{(1-m)}{m}\left(2 + \frac{\mu_\ell}{\mu_g}\,\frac{(1-m)}{m}\right)}\right] \tag{55}$$

$$\frac{Q_g}{Q_\ell} = \frac{(1-m)}{16\,m}\left(2 + \frac{\mu_\ell}{\mu_g}\,\frac{(1-m)}{m}\right) \tag{56}$$

One further relationship which is needed is the experimental relationship for (U_S/U_B). It can be stated in functional form as:

$$\frac{U_S}{U_B} = f\left(\frac{\mu_\ell\, U_S}{\sigma}\,,\ \lambda\right) \tag{57}$$

Equations (55), (56), and (57) are three equations in six unknowns. If we specify two of the parameters, solutions of the equations can be plotted on two dimensions. It is convenient to specify the parameters λ and (μ_ℓ/μ_g). Then we can plot $(\mu_\ell\ U_S/\sigma)$ versus $(1/1 + Q_g/Q_\ell)$ or equivalently $(Q_\ell/Q_g + Q_\ell)$ for the solution to

(55), (56), and (57). This has been done for λ equal to 1.5×10^{-5} and (μ_ℓ / μ_g) equal to 25 and 50. The solution is plotted on Figs. 18 and 19.

Experiments were performed to test the validity of this flow boundary. The conditions were those which are shown inFigs. 18 and 19. Water and nitrogen and heptane and nitrogen were tested in tubes of 0.0795 centimeters nominal radius. The flow was observed visually and with a camera. Slug flow was said to exist if a slug would occasionally pass through. If not, the flow was considered annular. The photographs showed that when slugs became very far apart and when annular flow existed the effects of gravity were quite strong. The annular flow became somewhat of a stratified flow. Also small waves occurred on the surface of the film. Even with these disturbances the data for annular flow and slug flow fell approximately as would be expected from the analysis. The data for these experiments are shown on Figs. 18 and 19. The scatter of the data is not bad when one considers all the side effects which occurred. These experimental results lead to the conclusion that an annular or stratified annular flow boundary does exist to slug flow and it can be reasonably well predicted.

The other boundary to slug flow appears to be a break up of the tails of the bubbles. Experiments show that the tails of the bubbles in slug flow begin to break up at some critical bubble velocity. This flow with small bubbles at the tails of the larger bubbles is called bubbly slug flow. When the velocity is increased much further than the critical velocity, the tiny bubbles fill the slug and begin to deform the large bubbles behind them. This eventually degenerates into a bubbly or frothy flow when the velocity is increased to a sufficient degree. The order of magnitude where frothy or bubbly flow occurs is around twice the critical velocity. The primary concern here is the transition to a bubbly slug flow. The others are important but they constitute another problem.

The break up of a slug flow to bubbly slug flow appears to be a phenomenon where the surface tension forces at the tail of a bubble are overcome by a combination of inertia forces and viscous forces. For this reason it was thought possible to correlate the data for transition with only three parameters at the maximum. These parameters should include the three forces involved and the geometry of a slug. The bubble length, gas viscosity and gravity were thought to be unimportant. The parameters chosen were a Weber Number, N_{We}, and $(\sigma_S / \pi r_o^3)$. The Weber Number is defined as:

$$N_{Web} = \frac{\rho_\ell U_B^2 r_o}{\sigma} \tag{58}$$

A set of experiments was carried out to determine the boundary. The experimental procedure was just as for slug flow except that the photographs of the bubbles were taken from a closer position. The break up to bubbly slug flow was determined from the photographs. A photograph of a bubbly slug flow is shown on Fig. 6. The experimental data are indicated on Fig. 20.

The plot of Fig. 20 does not have $(\mathcal{V}_S/\pi r_o^3)$ as a parameter as would be indicated from the previous discussions. In one system, Test 71, the effect of $(\mathcal{V}_S/\pi r_o^3)$ on the boundary was tested. It was found that there is very little effect. Therefore the plot was made without taking $(\mathcal{V}_S/\pi r_o^3)$ into account.

The data indicates that the plot takes the proper parameters into account. The data for water and nitrogen and heptane and nitrogen in a 0.0795 centimeter nominal radius tube, which have quite different values of Ω and (μ_ℓ/μ_g), show little dependence on them for transition. The bubble length was randomly varied in these experiments and again appeared to have little significance.

According to at least one theory, the density of the gas should be a factor in the break up to bubbly or frothy flow. Since the bubbly slug flow appears to be a transition between slug and bubbly or frothy flow, it might be suspected that gas density is important. For this reason, a test, Test 72, was run to determine the effects of a much lighter gas (helium). The transition occurred in much the same place as for the data with a heavier gas (nitrogen). This verified that it is correct to ignore gas density in determining the bubbly slug flow boundary.

The boundary of Fig. 20 is not a sharp one. This is not too surprising since the transition might be expected to go according to a stability criterion. It definitely does not appear to be a pure Weber Number effect. A line that passes through the middle of the transition region is one which is given by:

$$(N_{Re}) \times (N_{Web}) = 2.8 \times 10^{+5} \tag{59}$$

Equation (59) should be used only in the range of λ shown on Fig. 20. There is no reason to believe that it applies outside of that range.

Equation (56) represents a flow regime boundary. However, it is not in a very convenient form. It would be preferable if it were given in terms of the parameters for the annular flow boundary; then they could all be placed on one flow map. This is easily done, for we can say for the boundary:

$$(N_{Re}) \times (N_{Web}) = \frac{\Psi^3}{\lambda^2} = 2.8 \times 10^{+5} \qquad (60)$$

Thus given a value of λ, we can find Ψ for transition and therefore (U_S/U_B) and $(\mu_\ell U_S/\sigma)$. There is no dependence on $(Q_\ell/Q_g + Q_\ell)$ for this transition. A plot of this boundary for $\lambda = 1.5 \times 10^{-5}$ is given on Fig. 21 along with the annular flow boundary where $(\mu_\ell/\mu_g) = 50$.

On Fig. 21 the different regimes of flow are indicated. The boundary between annular and bubbly slug flow should be about as shown but its upper limit is unknown. This figure indicates only the possibility of slug flow. The actual existence of slug flow can only be determined from the inlet conditions. A flow regime map such as Fig. 21 completely specifies the boundaries for a type of horizontal capillary slug flow when used in conjunction with (52), (53) and (54).

4.6. Application of Results

In a typical two phase flow problem the following information is available:

1. Magnitude of gravity field, g.
2. Orientation of tube from vertical, θ.
3. Tube size, r_o, L.
4. Flow rate of liquid and gas, Q_ℓ and Q_g.
5. Liquid and gas properties, ρ_ℓ, ρ_g, μ_ℓ, μ_g and σ.

In this section it is shown what answers are available from this work to a problem specified as above, and how those answers are obtained.

The first question to be answered is whether horizontal capillary slug flow exists or not. If this question is not answered affirmatively, little else can be gained from this work. The parameters to be calculated and the requirements on some of them for horizontal capillary slug flow to be possible are as follows:

1. $\theta = 90^{o}$

2. $\mu_{\ell}/\mu_{g} > 25$

3. $\rho_{\ell}/\rho_{g} \gg 1$

4. $\Omega = \rho_{\ell} g r_{o}^{2}/\sigma < 0.22$

5. $\lambda = \mu_{\ell}^{2}/\rho_{\ell}\sigma r_{o}$

6. $\mu_{\ell} U_{S}/\sigma$

7. $Q_{\ell}/Q_{\ell} + Q_{g}$

If the first four requirements are met, a flow regime map may be drawn from the values of (2) and (5). The flow regime map is drawn as shown in Sec. 4.5 of this chapter on a plot of parameters (6) and (7). Then if the values of (6) and (7) fall within the region of slug flow on the flow map, horizontal capillary slug flow may exist. Actual slug flow depends on inlet conditions, but for the sake of discussion it is assumed that under these conditions slug flow does exist. The validity of the flow map depends to a large extent on the value of λ. If it is greatly different from the values tested here, the boundary is not likely to be valid. The more sensitive boundary in this respect is the boundary to bubbly slug flow.

If slug flow does exist, there are several properties of the flow which can be calculated. The most accurate calculation which can be made is density. The density may be calculated from (U_S/U_B) and the flow rates Q_{ℓ} and Q_g. The value of (U_S/U_B) is found from the value of $(\mu_{\ell} U_S/\sigma)$ and Fig. 17. These calculations for density are valid if Q_{ℓ} and Q_g are uniformly distributed in time.

The pressure drop can be calculated if the distribution of bubble and slug lengths is known. If this is not known, only an approximation can be made. To see what the pressure drop can vary over, we examine the possible variations in slug length. It can be shown that the ratio of the sum of all the bubble lengths in a tube to the sum of all the slug lengths is approximately equal to the ratio of gas to liquid flow rates, if the flow is somewhat uniform in time. This is the same restriction as for the density. Now this means that for given flow rates the sum of the slug lengths remains constant. The pressure drop correlations

all have a term which is linear with $(\mathcal{V}_S/\pi r_o^3)$ or equivalently (L_S/r_o). This part of the pressure drop is fixed for a given flow. The end effects of the bubbles and other terms which are not dependent on slug length all act per slug. Thus the fewer the bubbles and slugs, the lower the total pressure drop. An arbitrary minimum number of bubbles and slugs may be set at one bubble and slug per tube length. This gives a minimum pressure drop. This is not as useful as a maximum pressure drop but it can be considered as one limit. An alternate procedure would be to experimentally correlate bubble and slug lengths for a given process such as boiling or condensing.

The film thickness near the nose of the bubble may be calculated near the noses of the bubbles from equations (31) or (C5) and (32). If the value of another parameter τ is not too large as judged from Fig. A3, this should also be the film thickness near the tail.

Even if τ is large enough to cause a large amount of drainage, the value of (1-m) as determined at the nose should still be about the same at the tail.

4.7. Comparison with Other Correlations

The work here allows one to predict the horizontal capillary slug flow regime and to calculate pressure drop, density and film thickness under certain restrictions. Of these, pressure drop, density, and to some extent film thickness can be compared with other correlations.

The pressure drop is compared to the work of Lockhart and Martinelli[13]. The difference in approaches to the problem makes it difficult to compare, in general, but Regions I and II of the pressure drop correlations can be compared with some ease. The flow is assumed to be of uniform bubble and slug length for the comparison.

Regions I and II fall within the Lockhart-Martinelli regime of viscous-viscous flow. If the gas and the liquid were flowing in the tube independently, the flow would be laminar. One method of using the Lockhart-Martinelli correlations is to use the definition:

$$\left(\frac{\Delta P}{\Delta \frac{x}{r_o}}\right)_{TP} = \phi_{\ell vv}^{\,2} \left(\frac{\Delta P}{\Delta \frac{x}{r_o}}\right)_{\ell} \tag{61}$$

where the $(\Delta P/\Delta\, x/r_o)_\ell$ is the pressure gradient for the liquid flowing alone. The function $\phi_{\ell vv}$ is characteristic of viscous-viscous flow and in turn is correlated as a function of another parameter X. For viscous-viscous flow, X is defined as:

$$X = \frac{Q_\ell}{Q_g}\,\frac{\mu_\ell}{\mu_g} \tag{62}$$

The pressure drop in Region II is given by:

$$\frac{\frac{\Delta P}{\mu_\ell U_B}}{r_o} = 8\,\frac{\mathcal{V}_S}{\pi r_o^{\,3}} + 0.163\,\frac{\rho_\ell U_B\, r_o}{\mu_\ell} \tag{63}$$

where the pressure drop is over a length $(L_S + L_B)$. The average pressure gradient should be:

$$\frac{\dfrac{\Delta P}{\left(\dfrac{L_S + L_B}{r_o}\right)\dfrac{\mu_\ell U_B}{r_o}}}{} = \frac{\dfrac{8\mathcal{V}_S}{\pi r_o^3} + 0.163\ \dfrac{\rho_\ell U_B r_o}{\mu_\ell}}{\dfrac{L_S + L_B}{r_o}} \tag{64}$$

Let us compare the Lockhart-Martinelli pressure gradient with that of equation (64) by using the ratio of the two. Call this ratio Z.

$$Z = \frac{\phi_{\ell vv}^2 \left(\dfrac{\Delta P}{\Delta \dfrac{x}{r_o}}\right)_\ell}{\left(\dfrac{8\mathcal{V}_S}{\pi r_o^3} + 0.163\ \dfrac{\rho_\ell U_B r_o}{\mu_\ell}\right)\left(\dfrac{\mu_\ell U_B}{r_o}\right)} \Bigg/ \frac{L_S + L_B}{r_o} \tag{65}$$

Equation (65) can be simplified by use of the following relationships:

$$\left(\frac{\dfrac{\Delta P}{x}}{\Delta \dfrac{x}{r_o}}\right)_\ell = \frac{8\,\mu_\ell\, Q_\ell}{\pi r_o^3} \tag{66}$$

for laminar flow.

$$Q_\ell = \frac{\mathcal{V}_S\, U_B}{L_S + L_B} \tag{67}$$

Equations (66) and (67) can be combined to get:

$$\left(\frac{\dfrac{\Delta P}{x}}{\Delta \dfrac{x}{r_o}}\right)_\ell = \frac{8\mu_\ell}{\pi r_o^3}\ \frac{\mathcal{V}_S U_B}{\left(L_S + L_B\right)} \tag{68}$$

Equation (68) can be substituted into equation (65) to get:

$$Z = \frac{\phi_{\ell vv}^{2}}{1 + \dfrac{0.163\ \rho_\ell U_B r_o}{\mu_\ell} \Big/ \dfrac{8\mathcal{V}_S}{\pi r_o^{3}}} \tag{69}$$

Equation (70) could have been written for Region I as:

$$Z = \frac{\phi_{\ell vv}^{2}}{1 + \dfrac{45}{8\mathcal{V}_S / \pi r_o^{3}}} \tag{70}$$

The results of equation (69) are shown on Fig. 22. The value of (μ_ℓ/μ_g) is set at 50 and $(\rho_\ell U_B r_o/\mu_\ell)$ is set at 450. Z is plotted versus $(\mathcal{V}_S/\pi r_o^{3})$ with (Q_ℓ/Q_g) as a parameter. The ratio of the two is never very much greater than one. The ratio is one at fairly low values of $(\mathcal{V}_S/\pi r_o^{3})$. Notice that the lower value of (Q_ℓ/Q_g) crosses the value of one at a lower value of $(\mathcal{V}_S/\pi r_o^{3})$. It is reasonable that $(\mathcal{V}_S/\pi r_o^{3})$ is smaller for lower (Q_ℓ/Q_g).

The data and correlations for the Lockhart-Martinelli work are supposed to apply to flows other than slug flows. Yet if a reasonable approximation is made for the surface tension of their liquids, their data fall in the region of possible slug flow. It is quite likely that their flows were not true slug flows, but were of many small bubbles. This would imply short slugs. Therefore, the matching of the two correlations at low $(\mathcal{V}_S/\pi r_o^{3})$ is reasonable.

The density can also be compared to the work of Lockhart and Martinelli. Their parameter to measure density is the fraction of the total volume which is gas. This is called Rg. It can be shown that Rg can be stated in terms of the parameters used in the present work to be:

$$Rg = \frac{U_S}{U_B} \left(\frac{1}{\frac{Q_l}{Q_g} + 1} \right) \tag{71}$$

This is quite different from the correlation of Lockhart and Martinelli. Their correlation showed Rg to be a function of X only. X is a function of (Q_l/Q_g) and (μ_l/μ_g) as shown before. If we assume a value of (μ_l/μ_g), say 50, we can plot Rg from equation (72) versus X. (U_S/U_B) must be a parameter on this plot. This plot is shown on Fig. 23 with a value of (U_S/U_B) of 1.0 and 0.5. The Lockhart-Martinelli correlation for Rg is also shown on this figure. The comparison is reasonably good for values of X less than 6.5, but it is not good at all beyond this. The high value of Rg from Lockhart-Martinelli at X greater than 6.5 would imply that the density is less than that which would occur if the gas-liquid ratio in the tube were equal to the gas liquid flow ratio. This type of flow is difficult to conceive.

The film thickness of Fairbrother and Stubbs[6] is assumed to cause a limiting value on (U_S/U_B). The shape of the curve of (U_S/U_B) based on the Fairbrother-Stubbs film thickness is not too dissimilar to the curves measured here. Their curve appears to make a reasonable limiting value. This is no real comparison, of course, but it does show that there is no conflict of results.

5. SUMMARY AND CONCLUSIONS

When two phases flow in tubes of small diameter, quite often the gas flows as long bubbles separated from the wall by a film of liquid and separated from each other by slugs of liquid. Because of the small diameter of the tubes and the similarity to other flows called slug flows, this type of flow is called capillary slug flow. Capillary slug flow has been studied when it flows in a horizontal tube.

Pressure drop, density and, to a certain extent, film thickness have been correlated for a type of horizontal capillary slug flow. The conditions under which the flow exists and the correlations are valid have been defined. A horizontal slug flow satisfies the conditions of the definition if:

1. $\rho_\ell / \rho_g \gg 1$
2. $\mu_\ell / \mu_g > 25$
3. $\rho_\ell g r_o^2 / \sigma < 0.22$

Under these conditions the flow regime is still not necessarily a capillary slug flow. Depending on the gas and liquid flow rate, the flow may flow in other regimes. The regimes bounding capillary slug flow are annular flow for low liquid to gas flow ratios and bubbly slug flow for high throughput velocities.

Zero gravity flow can be included in the flow regime. In fact, this is the only case in which the film thickness may be calculated to any degree.

The effect of impurities in the liquid was studied to a small extent. It was found that the pressure drop is greatly changed by impurities.

The correlations developed here have been compared to other works. No significant differences were found which would indicate that this work is in great error. If anything, the comparison shows the reasons why other correlations work and why they do not.

The conclusions reached are as follows:

1. Given a horizontal two phase flow system, the existence of a capillary slug flow where the correlations and analyses here are valid can be determined.

2. If the flow does exist, the pressure drop, density, and, to a certain extent, film thickness can be accurately determined when the slug and bubble lengths are known. If these are not known, good approximations may be made for density and possibly film thickness, but only a lower limit can be placed on pressure drop.

NOMENCLATURE

g	acceleration of gravity
K	arbitrary function or constant
L	arbitrary length
L_S	length of slug
L_B	length of bubble
L_t	total length
m	fraction of tube cross-section covered with liquid film
N_{Fr}	Froude Number
N_{Re}	Reynolds Number
N_{Web}	Weber Number
p	pressure
p_B	pressure in a bubble
p_d	pressure defined by equation (A4)
p_f	pressure in a liquid film
p_g	pressure in gas core of annular flow
p_i	pressure in liquid at surface of bubble
ΔP	pressure drop across one bubble and slug
ΔP_B	pressure drop within a bubble
$\left(\Delta P/\Delta\, x/r_o\right)_{TP}$	Lockhart-Martinelli two phase pressure gradient
$\left(\Delta P/\Delta\, x/r_o\right)_{\ell}$	pressure gradient for liquid flowing alone
Q_g	average volume flow rate of gas
Q_{ℓ}	average volume flow rate of liquid
Q_{g1}	instantaneous gas flow rate at 1
$Q_{\ell 1}$	instantaneous liquid flow rate at 1
Q_S	instantaneous flow rate in a slug
r	radial polar coordinate from center of tube
r_a	radius to gas liquid interface in annular flow
r_B	radius of bubble
r_f	radius to liquid element in liquid film
r_g	radius to gas element in gas core
r_i	polar coordinate to inner surface of bubble

r_o	radius of tube
r'	polar coordinate centered on bubble
r_i'	polar coordinate to surface of bubble from center of bubble (equals r_B)
R_g	fraction of total volume which is gas
t	time
U_B	bubble velocity
U_S	velocity of liquid in slug
v_l	specific volume at l
V	arbitrary velocity
V_a	velocity of liquid-gas interface
V_f	velocity in liquid film
V_g	velocity in gas core of annular flow
V_r	velocity in radial direction
V_ϕ	velocity in tangential direction
$V_{\phi m}$	mean velocity in tangential direction
$\mathcal{V}_{g\ c.v.}$	volume of gas in control volume
$\mathcal{V}_{\ell\ c.v.}$	volume of liquid in control volume
$\mathcal{V}_B$	volume of gas in a bubble
$\mathcal{V}_{Bi}$	volume of gas in bubble i
$\mathcal{V}_S$	volume of liquid flowing per bubble and slug
x	distance along axis of tube
X	Lockhart-Martinelli parameter
y	distance of bubble rise
Z	ratio of Lockhart-Martinelli pressure gradient to gradient of correlation developed here
∇	operator del
Γ	arbitrary function in equation (50)
$\phi_{\ell vv}$	Lockhart-Martinelli parameter for viscous-viscous flow
ϕ	angle in polar coordinates measured at center of tube
ϕ'	angle in polar coordinates measured at center of bubble
Ψ	dimensionless parameter $(\mu_\ell U_B/\sigma)$
λ	dimensionless parameter $(\mu_\ell^2/\rho_\ell \sigma r_o$

Ω	dimensionless parameter ($\rho_\ell g r_o^2/\sigma$)
ρ_ℓ	density of liquid
ρ_g	density of gas
μ_ℓ	viscosity of liquid
μ_g	viscosity of gas
σ	surface tension
θ	angle of tube from vertical
τ	dimensionless parameter ($L_B \rho_\ell g r_o / U_B \mu_\ell$)

BIBLIOGRAPHY

1. Adam, N. K., "The Physics and Chemistry of Surfaces", Oxford University Press, Third Edition, 1941.

2. Adamson, A. W., "Physical Chemistry of Surfaces", Interscience Publishers, 1960.

3. Bikerman, J. J., "Surface Chemistry Theory and Applications", Academic Press, 1958.

4. Bretherton, F. B., "The Motion of Long Bubbles in Tubes", Journal of Fluid Mechanics, Vol. 19, Part 2, March 1961.

5. Cox, B. G., "On Driving a Viscous Fluid Out of a Tube", Journal of Fluid Mechanics, Vol. 14, September 1962.

6. Fairbrother, F., and Stubbs, A. E., Journal of Chemical Society 1, 527, 1935.

7. Goldsmith, H. L., and Mason, S. G., "The Flow of Suspensions Through Tubes II. Single Large Bubbles", Technical Report No. 247, Pulp and Paper Research Institute of Canada, August 1961.

8. Griffith, P., and Wallis, G. B., "Two Phase Slug Flow", ASME Paper No. 60-HT-28.

9. Handbook of Chemistry and Physics, Chemical Rubber Publishing Co., Thirty-Sixth Edition, 1954 - 1955.

10. Harkins, W. D., and Jordan, H. F., "A Method for the Determination of Surface and Interfacial Tension from the Maximum Pull on a Ring", Journal of American Chemical Society 52, 1751, 1930.

11. International Critical Tables, McGraw-Hill Book Co., 1928.

12. Lee, K. S., "An Experimental Dimensionless Correlation of Liquid Bubbles Rising in Capillary Tubes", Thesis (S. M.), Dept. of Mech. Engr., Mass. Inst. of Tech., June 1962.

13. Lockhart, R. W., and Martinelli, R. C., "Proposed Correlation of Data for Isothermal Two-Phase, Two-Component Flow in Pipes", Chemical Engineering Progress, Vol. 45, No. 1, January 1949.

14. Marchessault, R. N., and Mason, S. G., "Flow of Entrapped Bubbles Through a Capillary", Industrial Engineering Chemistry, Vol. 52, No. 1, January 1960.

15. Marcy, G. P., "Pressure Drop with Change of Phase in a Capillary Tube", Journal of ASRE, January 1949.

16. Moissis, R., "The Transition from Slug to Homogeneous Two Phase Flows", ASME Paper 62-H-48.

17. Nicklin, D. J., Wilkes, J. D., and Davidson, J. F., "Two Phase Flow in Vertical Tubes", Transactions of the Institute of Chemical Engineers, 1962.

18. Rohsenow, W. M., and Choi, H. Y., "Heat, Mass and Momentum Transfer", Prentice-Hall, August 1961.

19. Taylor, G. I., "Deposition of a Viscous Fluid on the Wall of a Tube", Journal of Fluid Mechanics, Vol. 10, Part 2, March 1961.

20. Whitesel, H. A., "Capillary Two Phase Flow, Part I", Refrigeration Engineering, April 1957.

APPENDIX A

Drainage Around a Bubble

As a bubble passes through a horizontal tube, it leaves a thin film of liquid on the wall. This film of liquid should drain to the bottom of the tube given sufficient time. The object of this appendix is to determine to what extent the film drains. An equivalent point of view is to determine how fast the bubble rises.

To get a measure of the drainage some assumptions must be made about the flow. These assumptions are listed below:

1. The viscosity ratio (μ_ℓ/μ_g) is very large so that the gas viscosity can be ignored in every respect.
2. The bubble is long and cylindrical enough that the arguments in Chapter 2 for zero axial flow are valid.
3. The bubble can be treated in only two dimensions. The surface tension effects in the axial direction are small as are any other coupling forces in the axial direction.
4. The liquid film is thin with respect to tube radius.
5. The bubble retains its cylindrical shape as it rises. This is reasonable when the ratio of gravity to surface tension forces is large.
6. The flow in the film is entirely tangential and all derivatives of velocity with respect to space and time are small compared to the derivative of tangential velocity with respect to the radial direction. Also the flow is non-inertial.

These assumptions allow us to look at a bubble at one point in the tube from the time a bubble nose goes by to the time the tail comes by. The liquid at that point drains or the bubble rises as a two-dimensional, time-dependent, non-inertial, viscous flow. A model for such a flow is given in Fig.(A1).

In Fig. (A1) the primed quantities are taken with respect to a coordinate system moving with the bubble center and the unprimed quantities are with respect to a fixed coordinate system. The subscript i represents conditions at the interface.

The continuity equation can be written for the model as:

$$V_{\phi m} = \int_{r_i}^{r_o} \frac{V_\phi \, dr}{(r_o - r_i)} = \frac{r_i \sin\phi}{(r_o - r_i)} \frac{dy}{dt} \tag{A1}$$

where $V_{\phi m}$ is the average velocity in the tangential direction at the angle ϕ at some arbitrary time.

The Navier-Stokes equations for the liquid in the film are:

$$\frac{\partial V_r}{\partial t} + V_r \frac{\partial V_r}{\partial r} + \frac{V_\phi}{r} \frac{\partial V_r}{\partial \phi} - \frac{V_\phi^2}{r}$$

$$= - \frac{1}{\rho_\ell} \frac{\partial P_d}{\partial r} + \frac{\mu_\ell}{\rho_\ell} \left(\nabla^2 V_r - \frac{V_r}{r^2} - \frac{2}{r^2} \frac{\partial V_\phi}{\partial \phi} \right) \tag{A2}$$

$$\frac{\partial V_\phi}{\partial t} + V_r \frac{\partial V_\phi}{\partial r} + \frac{V_\phi}{r} \frac{\partial V_\phi}{\partial \phi} + \frac{V_r V_\phi}{r}$$

$$= - \frac{1}{\rho_\ell r} \frac{\partial P_d}{\partial \phi} + \frac{\mu_\ell}{\rho_\ell} \left(\nabla^2 V_\phi + \frac{2}{r^2} \frac{\partial V_r}{\partial \phi} - \frac{V_\phi}{r^2} \right) \tag{A3}$$

where

$$\nabla^2 = \frac{\partial^2}{\partial r^2} + \frac{1}{r} \frac{\partial}{\partial r} + \frac{1}{r^2} \frac{\partial^2}{\partial \phi^2}$$

The term p_d is defined by the relation:

$$p = K - \rho_\ell g r \cos\phi + p_d \tag{A4}$$

where K is some constant and p is the actual pressure in the liquid. It is the difference between the actual pressure at a point and the pressure which would be there if there had been no motion.

The boundary conditions on (A2) and (A3) are:

$$\begin{aligned} &\text{at} \quad r = r_o, \; V_\phi = V_r = 0 \\ &\text{at} \quad r = r_i, \text{ shear stresses equal zero} \\ &\text{at} \quad \phi = 0, \; \pi, \; V_\phi, \; V_r = 0 \\ &\int_0^\pi p_i r_i' \cos\phi' \, d\phi' = - \frac{\rho_g g \pi r_i'^2}{2} \end{aligned} \tag{A5}$$

Assumption (6) allows equations (A2) and (A3) to be modified as:

$$\frac{\partial p_d}{\partial r} = - \frac{2\mu_\ell}{r^2} \frac{\partial V_\phi}{\partial \phi} \tag{A6}$$

$$\frac{\partial p_d}{\partial \phi} = r\mu_\ell \left(\frac{\partial^2 V_\phi}{\partial r^2} + \frac{1}{r} \frac{\partial V_\phi}{\partial \phi} - \frac{V_\phi}{r^2} \right) \tag{A7}$$

Assumption (4) allows any curvature effect to be eliminated. This gives us:

$$\frac{\partial p_d}{\partial \phi} = \mu_\ell r \frac{\partial^2 V_\phi}{\partial r^2} \tag{A8}$$

$$\frac{\partial p_d}{\partial r} = 0 \tag{A9}$$

Equation (A9) implies that p_d is independent of r and thus $\partial p_d/\partial \phi$ is also. Therefore, we can integrate equation (A8) with respect to r. The boundary condition of zero shear stress at the bubble interface can be stated as:

$$\frac{\partial V_\phi}{\partial r} = 0 \qquad \text{at} \quad r = r_i \tag{A10}$$

With this boundary condition the integrated result of (A8) is:

$$\left(\frac{\partial p_d}{\partial \phi}\right)\left(\ln \frac{r}{r_i}\right) = \mu_\ell \frac{\partial V_\phi}{\partial r} \tag{A11}$$

Equation(A11) can again be integrated with the boundary condition:

$$V_\phi = 0 \qquad \text{at} \quad r = r_o \tag{A12}$$

The result is:

$$r_i \left(\frac{\partial p_d}{\partial \phi}\right)\left[\frac{r_o}{r_i}\left(\ln \frac{r_o}{r_i} - 1\right) - \frac{r}{r_i}\left(\ln \frac{r}{r_i} - 1\right)\right] = -\mu_\ell V_\phi \tag{A13}$$

Equation (A13) can be substituted into (A1) to get:

$$\frac{r_i^2}{\mu_\ell (r_o - r_i)}\left(\frac{\partial p_d}{\partial \phi}\right)\left[\left(\ln \frac{r_o}{r_i}\right)\left(\frac{r_o}{r_i}\right)\left(1 - \frac{1}{2}\frac{r_o}{r_i}\right)\right.$$

$$\left. - \frac{r_o}{r_i}\left(1 - \frac{1}{4}\frac{r_o}{r_i}\right) + \frac{3}{4}\right] = \frac{r_i \sin\phi}{(r_o - r_i)} \frac{dy}{dt} \tag{A14}$$

Equation (A14) can be rearranged to give:

$$\frac{\partial p_d}{\partial \phi} = \frac{\mu_\ell \sin\phi \quad \frac{dy}{dt}}{r_i\left[\left(\ln \frac{r_o}{r_i}\right)\left(\frac{r_o}{r_i}\right)\left(1 - \frac{1}{2}\frac{r_o}{r_i}\right) - \frac{r_o}{r_i}\left(1 - \frac{1}{4}\frac{r_o}{r_i}\right) + \frac{3}{4}\right]} \tag{A15}$$

Equation (A15) can now be integrated with respect to ϕ:

$$p_d = \int_0^{\phi} \frac{\mu_\ell \sin\phi \quad \frac{dy}{dt} \quad d\phi}{r_i\left[\left(\ln \frac{r_o}{r_i}\right)\left(\frac{r_o}{r_i}\right)\left(1 - \frac{1}{2}\frac{r_o}{r_i}\right) - \frac{r_o}{r_i}\left(1 - \frac{1}{4}\frac{r_o}{r_i}\right) + \frac{3}{4}\right]} \tag{A16}$$

The pressure p_i of the boundary conditions can be written in terms of the primed parameters and K. To do this, use is made of the geometric relationship:

$$y + r_i' \cos\phi' = r_i \cos\phi \tag{A17}$$

Equation (A17) is substituted into equation (A4) to get:

$$p_i = K - \rho_\ell g (y + r_i' \cos\phi') + p_d \tag{A18}$$

Then the boundary conditions (A5) on p_i can be written:

$$\int_0^{\pi} \left[K - \rho_\ell g (y + r_i' \cos\phi') + p_d\right] r_i' \cos\phi' \, d\phi' = - \frac{\rho_g g \pi r_i'^2}{2} \tag{A19}$$

Equation (A19) can be reduced to:

$$\int_0^{\pi} p_d \, r_i' \cos\phi' \, d\phi' = \frac{\pi r_i'^2}{2} (\rho_\ell - \rho_g) g \tag{A20}$$

Equation (A16) and (A20) can be combined to obtain a relation for dy/dt.

$$\frac{dy}{dt} = \int_0^{\pi} \left[\int_0^{\phi} \frac{\sin\phi \, d\phi}{r_i \left[\left(\ln \frac{r_o}{r_i} \right) \left(\frac{r_o}{r_i} \right) \left(1 - \frac{1}{2} \frac{r_o}{r_i} \right) - \frac{r_o}{r_i} \left(1 - \frac{1}{4} \frac{r_o}{r_i} \right) + \frac{3}{4} \right]} \right] r_i' \cos\phi' d\phi' \qquad \frac{\pi r_i'^2}{2} \qquad \frac{(\rho_\ell - \rho_g) g}{\mu_\ell} \tag{A21}$$

dy/dt is the rise velocity of a bubble. It can be non-dimensionalized as follows:

$$\frac{d\left(\frac{y}{r_o}\right)}{d\left(\frac{\rho_\ell - \rho_g}{\mu_\ell} g r_o t\right)} = \frac{1}{\frac{r_o}{r_i'} \frac{2}{\pi} \int_0^{\pi} \left[\int_0^{\phi} \frac{\sin\phi \, d\phi}{\left(\ln \frac{r_o}{r_i} \right) \left(1 - \frac{1}{2} \frac{r_o}{r_i} \right) - \left(1 - \frac{1}{4} \frac{r_o}{r_i} \right) + \frac{3}{4} \frac{r_i}{r_o}} \right] \cos\phi' \, d\phi'} \tag{A22}$$

Equation (22) has no apparent closed form solution. The integrals of (A22) may be evaluated numerically from the geometric relationships:

$$\frac{r_i}{r_o} = \frac{y}{r_o} \cos\phi + \sqrt{\left(\frac{r_i'}{r_o}\right)^2 - \left(\frac{y}{r_o}\right)^2 \sin^2\phi} \tag{A23}$$

$$\phi = \cot^{-1} \left[\frac{\left(\frac{y}{r_o}\right)\left(\frac{r_o}{r_i'}\right) + \cos\phi'}{\sin\phi'} \right] \tag{A24}$$

The integrals are dependent on (y/r_o) and (r_i'/r_o) and give a dimensionless rise velocity as a function of these two parameters. The rise path of a bubble can be calculated in a stepwise manner from the dimensionless velocities. The rise path of a bubble has been calculated for the case of $(r_i'/r_o) = 0.80$ assuming that the bubble is initially centered. Notice that r_i' is equivalent to r_B in the text. Thus the plot can be said to be for $(1 - m) = 0.64$. This

solution is shown on Fig. A2. The path was calculated on a (y/r_o) increment of 0.05. The path was also calculated using only the initial rise velocity. It can be seen that not too bad an estimate is gained for the rise time using only this one step. The form of equation (A22) is much simplified for the case where the bubble is centered, for then $\phi = \phi'$ and $r_i = r_i'$. Equation (A22) becomes:

$$\frac{d\left(\frac{y}{r_o}\right)}{d\left(\frac{\rho_\ell - \rho_g}{\mu_\ell} g r_o t\right)} = \frac{\left(\ln \frac{r_o}{r_i'}\right)\left(1 - \frac{1}{2}\frac{r_o}{r_i'}\right) - \left(1 - \frac{1}{4}\frac{r_o}{r_i'}\right) + \frac{3}{4}\frac{r_i'}{r_o}}{\frac{r_o}{r_i'} \quad \frac{2}{\pi}\int_0^{\pi}\left(\int_0^{\phi'} \sin\phi' \, d\phi'\right) \cos\phi' \, d\phi'} \tag{A25}$$

The integrals in (A25) are easily integrated and (A25) becomes:

$$-\frac{d\left(\frac{y}{r_o}\right)}{d\left(\frac{\rho_\ell - \rho_g}{\mu_\ell} g r_o t\right)} = \frac{\left(\ln \frac{r_o}{r_i'}\right)\left(1 - \frac{1}{2}\frac{r_o}{r_i'}\right) - \left(1 - \frac{1}{4}\frac{r_o}{r_i'}\right) + \frac{3}{4}\frac{r_i'}{r_o}}{\frac{r_o}{r_i'}} \tag{A26}$$

Using equation (A26) for the rise velocity of a bubble, the paths of bubbles at various values of (r_i'/r_o) were calculated assuming they started at the center. They too are shown on Fig. A2.

The time available for a bubble to rise is equal to (L_B/U_B). Define a dimensionless time τ as:

$$\tau = \frac{L_B}{U_B} \quad \frac{(\rho_\ell - \rho_g) g r_o}{\mu_\ell} \tag{A27}$$

This should be a measure of the bubble drainage. The value which it has when the tail of a bubble just reaches the top is calculated from equation (A26). This is plotted as a function of (1 - m) on Fig. A3. Note that ρ_g is ignored in the coordinates of A2 and A3. This is in keeping with the assumptions $(\rho_\ell/\rho_g) >> 1$ in the text.

Notice that this method of calculation should indicate shorter rise times than a more thorough solution. It is not proposed as a good solution to bubble drainage rate but only as a means of determining if the effects of drainage may be significant. Also in the actual case the system would be complicated with the gas viscosity effects.

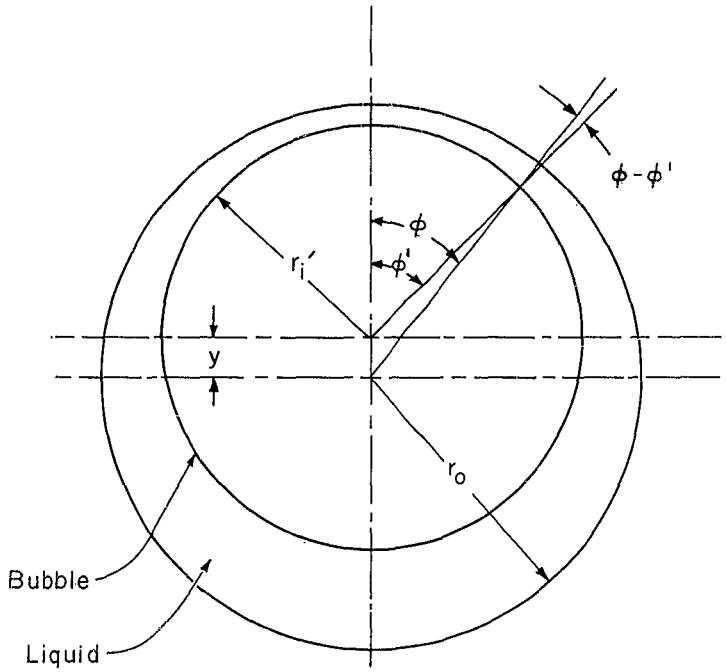

MODEL FOR BUBBLE RISE

FIGURE A-1

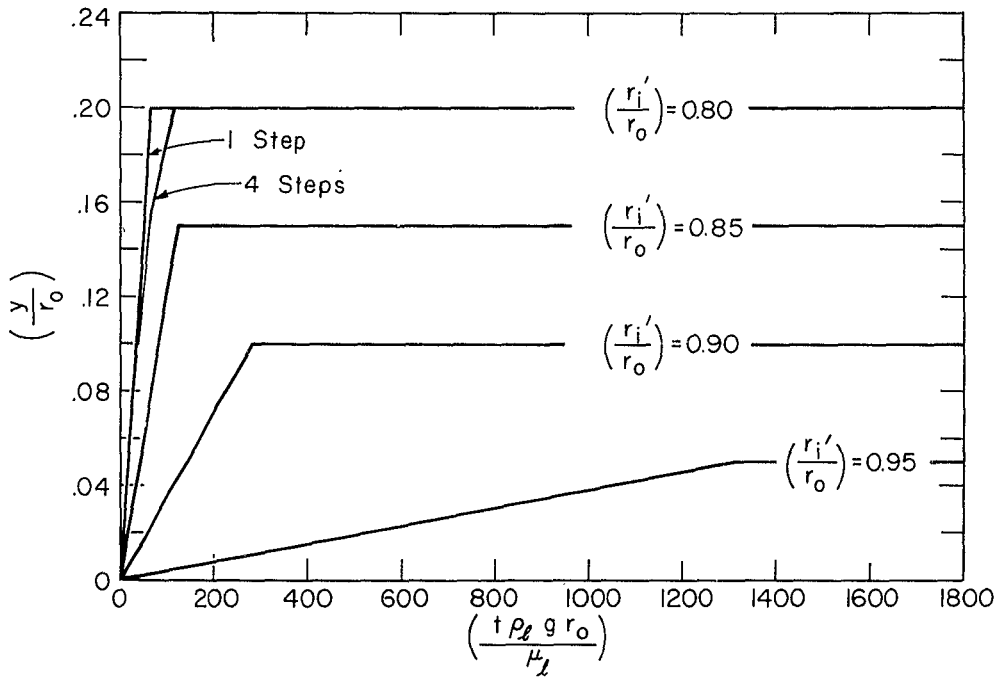

BUBBLE DRAINAGE PATH

FIGURE A-2

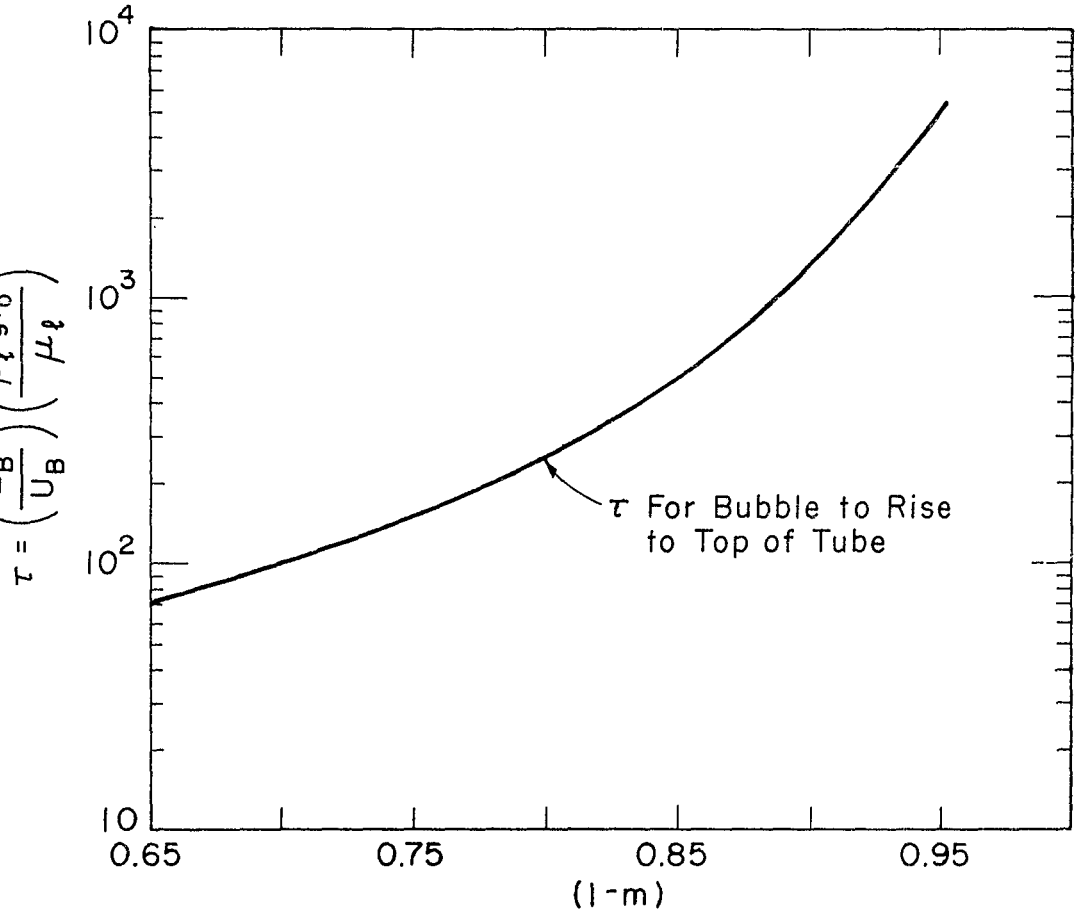

BUBBLE RISE TIME

FIGURE A3

APPENDIX B

Flow in an Annular Liquid Film

Take an annular liquid film as in Fig. B1. Make the assumptions that:

1. The gas and liquid are in laminar incompressible flow.
2. There is no slip at the liquid-gas boundary.
3. The flow is entirely axial.
4. The flow is axisymmetric, or free of gravitational effects.
5. The annulus radius r_a is constant with x.
6. The interface is stable (no waves).

If the gas were inviscid, there would be no shear on the interface. The finite viscosity of the gas does create a finite shear stress, however. This shear stress can be considered to cause the liquid to flow. The amount of this flow is to be calculated here under the assumptions given above.

The pressure gradient in the liquid is the same as the pressure gradient in the gas at a given x. There are two reasons for this. The first is that assumption 3 allows pressure gradients only in the axial direction. The second is that the pressure in the gas and liquid at the interface at a given x is given by:

$$p_f - p_g = - \frac{\sigma}{r_a} \tag{B1}$$

The subscript f refers to the film and the subscript g refers to the gas core. Since r_a is a constant, we can say:

$$\frac{dp_f}{dx} = \frac{dp_g}{dx} \equiv \frac{dp}{dx} \tag{B2}$$

The laminar flow equation for flow in tubes gives us:

$$V_g - V_a = \frac{1}{4\mu_g} \left(\frac{dp}{dx}\right) \left(r_g^2 - r_a^2\right) \tag{B3}$$

$$V_f = \frac{1}{4\mu_\ell} \left(\frac{dp}{dx}\right)\left(r_f^2 - r_o^2\right) \tag{B4}$$

The volume flow rates of liquid and gas can be expressed as:

$$Q_g = \int_0^{r_a} 2\pi r_g V_g \, dr_g \tag{B5}$$

$$Q_\ell = \int_{r_a}^{r_o} 2\pi r_f V_f \, dr_f \tag{B6}$$

Equation (B3) and (B4) can be substituted into (B5) and (B6) respectively to get:

$$Q_g = \pi \left[V_a r_a^2 - \frac{1}{8\mu_g} \left(\frac{dp}{dx}\right) r_a^4\right] \tag{B7}$$

$$Q_\ell = - \frac{2\pi}{\mu_\ell} \left(\frac{dp}{dx}\right) \left(r_o^2 - r_a^2\right)^2 \tag{B8}$$

A special case of equation (B4) is when $r_f = r_a$. In this case, we can write equation (B4) as:

$$V_a = \frac{1}{4\mu_\ell} \left(\frac{dp}{dx}\right)\left(r_a^2 - r_o^2\right) \tag{B9}$$

The term (dp/dx) can be eliminated in (B7) and (B8) by use of (B9). Equations (B7) and(B8) can then be written:

$$Q_g = \pi V_a r_a^2 \left(1 + \frac{1}{2} \frac{\mu_\ell}{\mu_g} \frac{r_a^2}{r_o^2 - r_a^2}\right) \tag{B10}$$

$$Q_\ell = 8\pi V_a (r_o^2 - r_a^2) \tag{B11}$$

Equations (B10) and B11) can be combined to get

$$\frac{Q_g}{Q_\ell} = \frac{1}{8} \frac{r_a^2}{r_o^2 - r_a^2} + \frac{1}{16} \frac{\mu_\ell}{\mu_g} \frac{r_a^4}{\left(r_o^2 - r_a^2\right)^2} \tag{B12}$$

We can use a definition of m of:

$$m = 1 - \frac{r_a^2}{r_o^2} \tag{B13}$$

It is seen that this m is exactly the same as used in the text when r_B was used. In this case r_a and r_B are equivalent. Using the definition (B13), equation (B12) can be simplified to:

$$\frac{Q_g}{Q_\ell} = \frac{1}{16} \frac{(1 - m)}{m} \left[2 + \frac{\mu_\ell}{\mu_g} \frac{(1 - m)}{m}\right] \tag{B14}$$

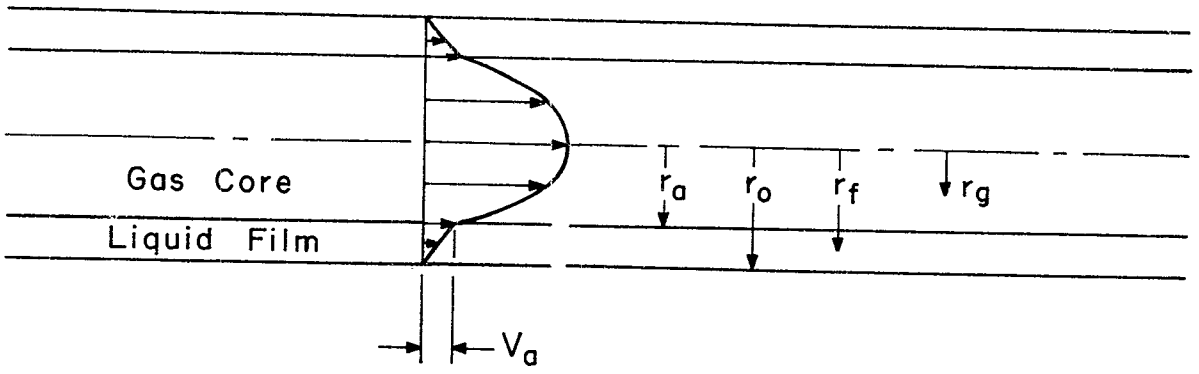

MODEL FOR ANNULAR FLOW

FIGURE BI

APPENDIX C

Relationship of Film Thickness to Velocity Ratio

In this Appendix the cross-sectional area of liquid around a bubble is calculated. The flow is as in Fig. C1. The analysis is based on the assumptions that the analysis of Appendix B is valid away from the bubble nose and tail. In this analysis the terms $Q_{\ell 1}$, Q_{g1}, and r_B are substituted for Q_ℓ, Q_g, and r_a respectively in the analysis of Appendix B. m then has the same meaning as it does in the text with the restriction that this value of m is valid only for a symmetric film.

The continuity equation tells us that for a steady bubble velocity and steady slug velocity:

$$Q_S = Q_{\ell 1} + Q_{g1} = Q_\ell + Q_g \tag{C1}$$

$$U_S = \frac{Q_s}{\pi r_o^2} \tag{C2}$$

$$U_B = \frac{Q_{g1}}{(1 - m)\, \pi r_o^2} \tag{C3}$$

Equations (C1), (C2), (C3) can be combined to give:

$$\frac{U_S}{U_B} = (1 - m)\left(1 + \frac{Q_{\ell 1}}{Q_{g1}}\right) \tag{C4}$$

Equation (B14) can be substituted into (C4) to get:

$$\frac{U_S}{U_B} = (1 - m)\left[1 + \frac{16}{\frac{(1 - m)}{m}\left(2 + \frac{\mu_\ell}{\mu_g}\frac{(1 - m)}{m}\right)}\right] \tag{C5}$$

It can be seen that equation (C5) reduces to the value as given by equation (31) in the text if (μ_ℓ / μ_g) is very large. This is some confirmation of the validity of the results. The relationship (C5) has been calculated for (μ_ℓ / μ_g) equal to 25 and 50. The resultant plot is shown on Fig. C2.

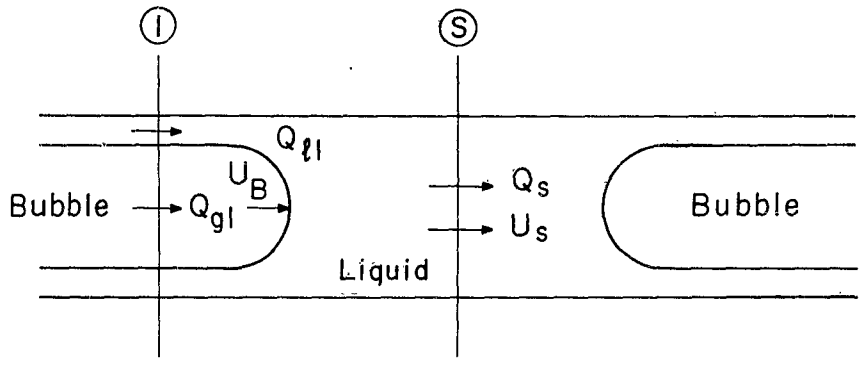

FLOW MODEL FOR FILM THICKNESS

FIGURE C1

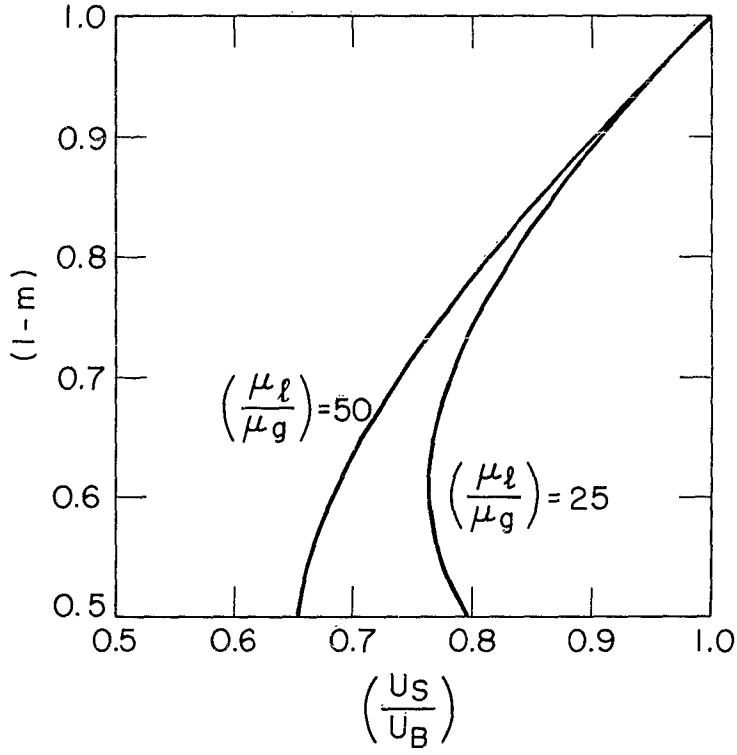

BUBBLE AREA AS A FUNCTION OF VELOCITY RATIO

FIGURE C2

APPENDIX D

Data Conditions for Figures 7 through 15

Test	Liquid	Gas	Tube radius cm	$\lambda \times 10^{+5}$	(μ_ℓ / μ_g)	Ω
28	Water	Air	0.0513	2.0-2.1	48-49	0.036
30	Water	Air	0.0513	2.0	47-48	0.036
31	Water	Air	0.0520	2.0-2.1	48	0.037
33	Water	Air	0.0520	2.0-2.1	48-49	0.037
34	Water	Air	0.0513	2.0-2.4	47-53	0.036
37	N-Heptane	N_2	0.0513	2.2-2.3	24-25	0.090
38	N-Heptane	N_2	0.0513	2.2	24	0.090
39	N-Heptane	N_2	0.0513	2.3	25	0.090
42	Water	Air	0.0513	2.1-2.2	48-50	0.036
43	Water	Air	0.0513	2.0-2.2	48-49	0.036
44	Water	Air	0.0513	2.1-2.3	49-50	0.036
45	Water	Air	0.0513	2.0-2.1	48-49	0.036
46	N-Heptane	N_2	0.0513	2.1	24	0.091
47	N-Heptane	N_2	0.0513	2.1	24	0.091
48	Water	Air	0.0793	1.5	51	0.085
49	Water	Air	0.0793	1.4	49	0.085
50	Water	Air	0.0793	1.3-1.5	47-50	0.085
51	Water	Air	0.0793	1.5-1.6	51-52	0.085
52	Water	Air	0.0793	1.4-1.6	49-52	0.085
53	Water	Air	0.0793	1.3-1.4	48	0.085
54	Water	Air	0.0793	1.4	49	0.085
55	Water	N_2	0.0793	1.4-1.6	52-55	0.085
56	Water	N_2	0.0793	1.5	52-53	0.085
57	Water	N_2	0.0802	1.4	52-53	0.088
58	Water	N_2	0.0802	1.3-1.4	51-52	0.088
59	Water	N_2	0.0516	2.2-2.5	51-56	0.036
60	Water	N_2	0.0516	2.3	53	0.036
62	N-Heptane	N_2	0.0516	2.3	25	0.090
64	N-Heptane	N_2	0.0802	1.5	25	0.22
65	N-Heptane	N_2	0.0802	1.5	25	0.22

66	N-Heptane	N_2	0.0802	1.5	26	0.22
67	N-Heptane	N_2	0.0802	1.5	25-26	0.22
69	Water	N_2	0.0802	1.7	58	0.087
70	Water	N_2	0.0802	1.3	49-50	0.088
71	N-Heptane	N_2	0.0516	2.1	23-24	0.091
72	N-Heptane	He	0.0516	2.1-2.2	23-24	0.091-0.092
73	N-Heptane	N_2	0.0516	2.1	23	0.092
74	N-Octane	N_2	0.0516	3.4	29-30	0.085

APPENDIX E

Figures

Fig.

APPENDIX E

Figures

Fig.

20. Flow Boundary, Slug to Bubbly Slug Flow

21. Flow Regime Map

22. Comparison of Lockhart-Martinelli Pressure Drop to This Correlation

23. Comparison of Void Volume to Lockhart and Martinelli

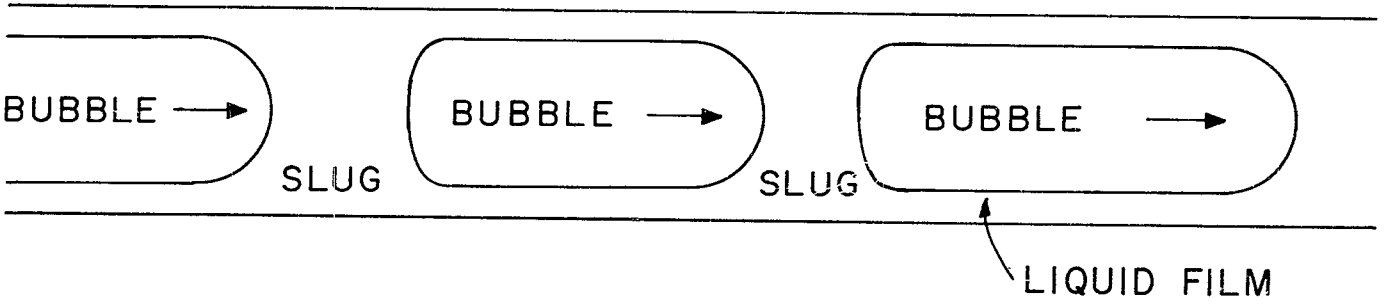

CAPILLARY SLUG FLOW

FIGURE 1

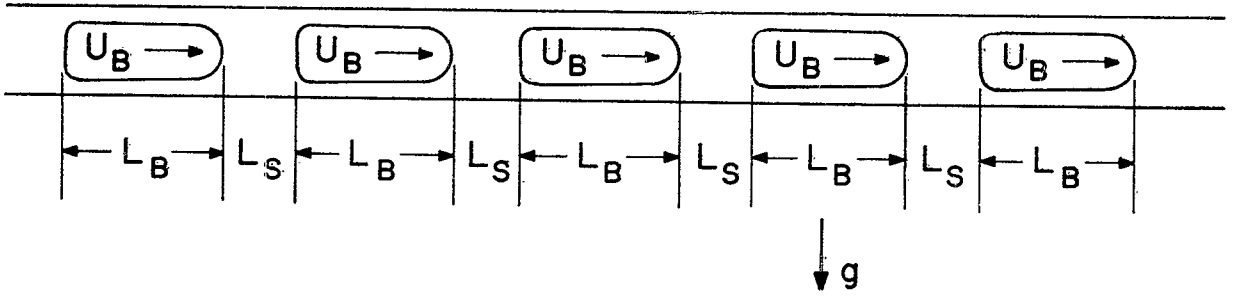

UNIFORM BUBBLE AND SLUG LENGTH
MODEL OF CAPILLARY SLUG FLOW

FIGURE 2

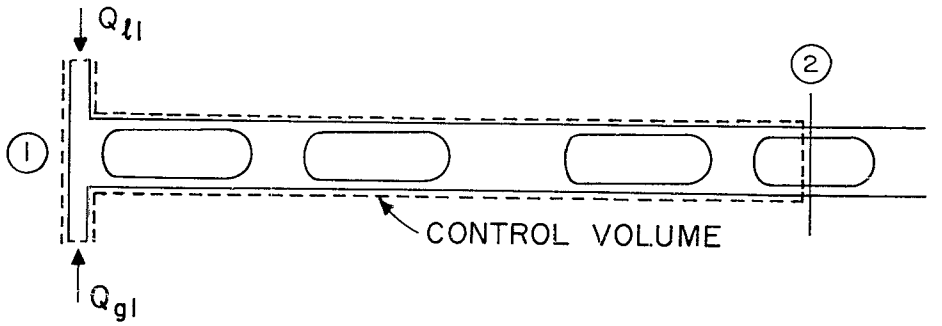

MODEL FOR CONTINUITY EQUATION

FIGURE 3

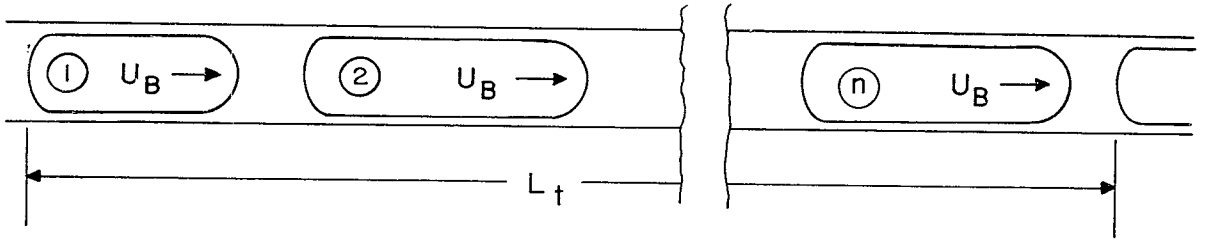

MODEL FOR DENSITY WITH
NON-UNIFORM L_S AND L_B

FIGURE 4

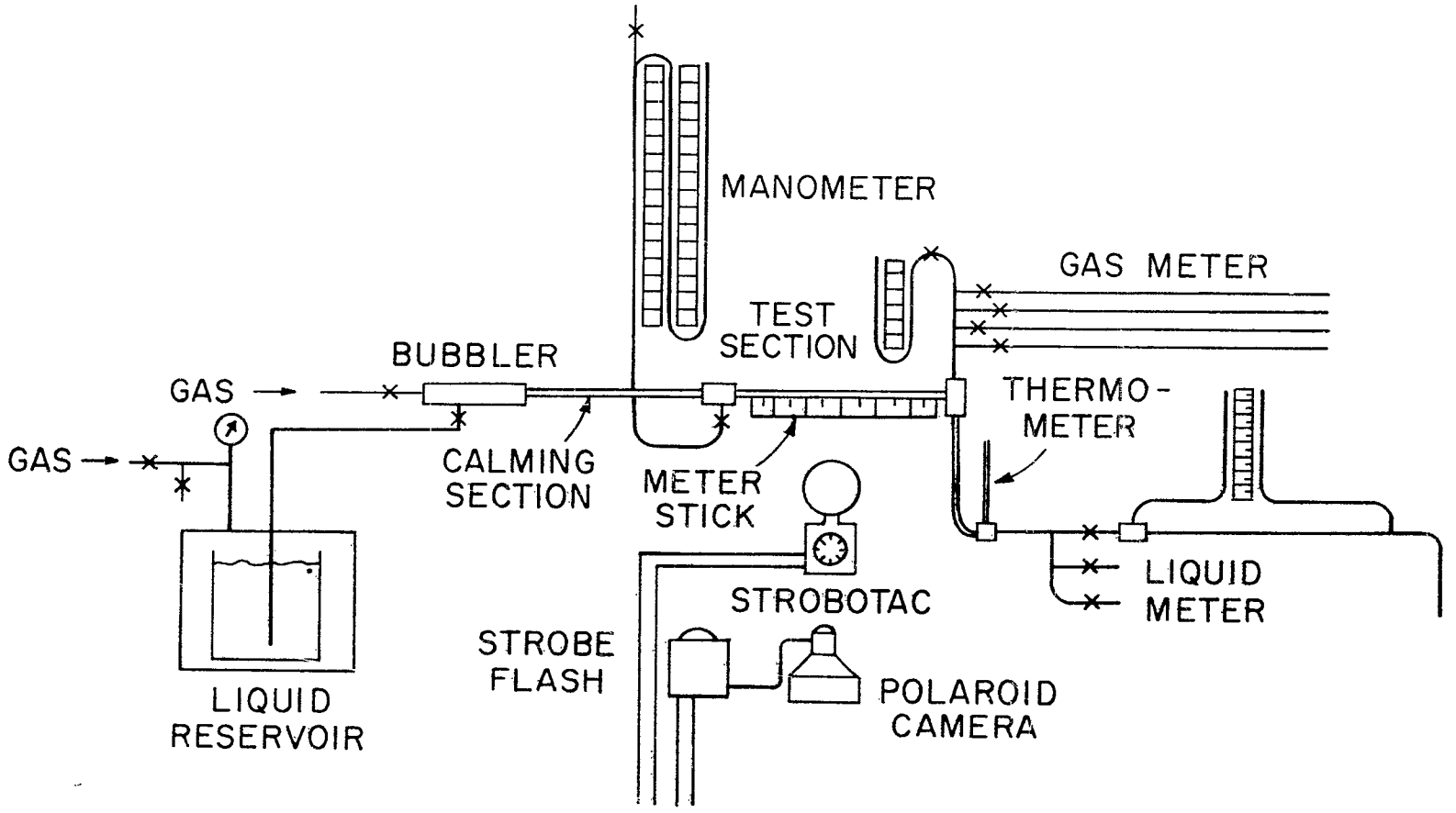

SCHEMATIC DIAGRAM OF EXPERIMENTAL APPARATUS

FIGURE 5

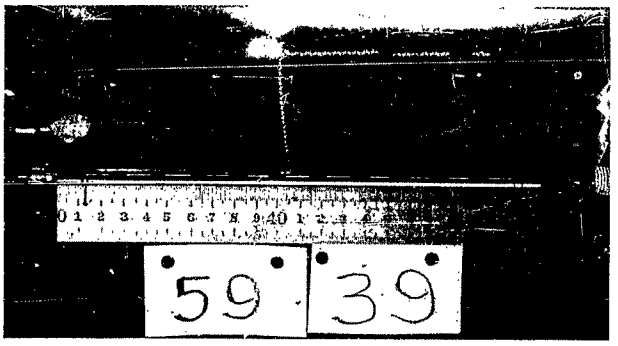

SLUG FLOW

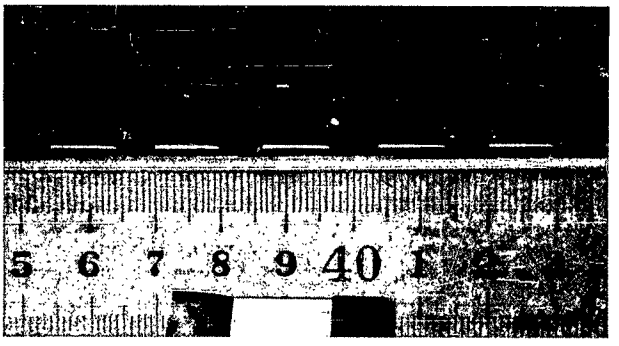

SLUG FLOW

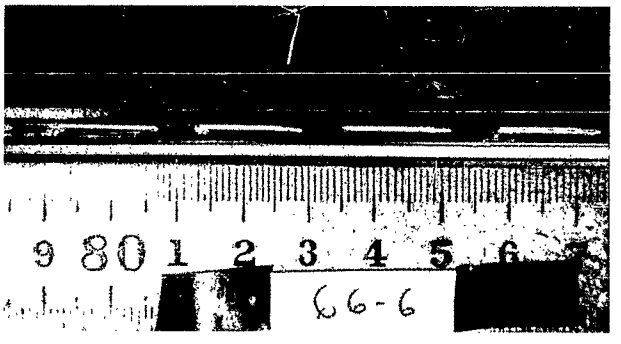

BUBBLY SLUG FLOW

PHOTOGRAPHS OF FLOW

FIGURE 6

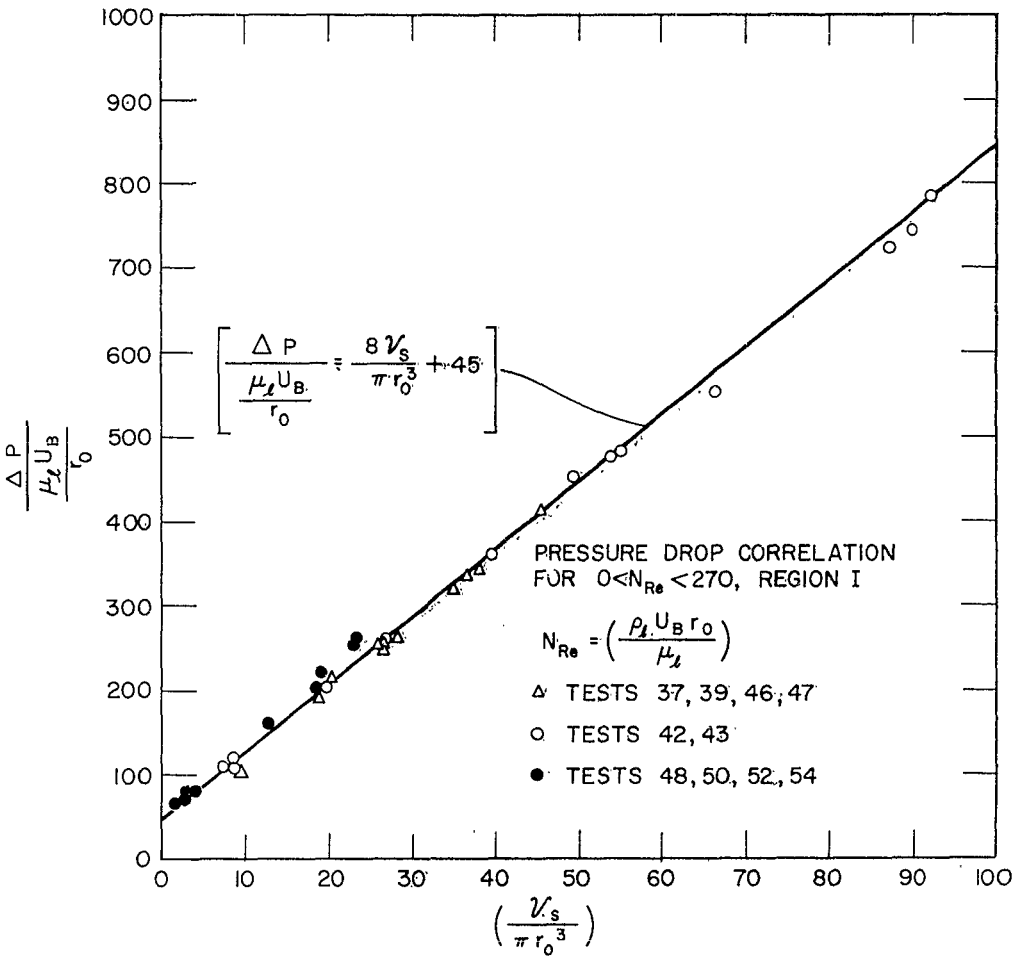
1000
900
800
700
600
500
400
300
200
100
0
0
10
20
30
40
50
60
70
80
90
100
$\frac{\Delta P}{\mu_l U_B / r_0}$
$\left(\frac{V_s}{\pi r_0^3}\right)$
$\left[\frac{\Delta P}{\mu_l U_B / r_0} = \frac{8 V_s}{\pi r_0^3} + 45\right]$
PRESSURE DROP CORRELATION
FOR $0 \leq N_{Re} < 270$, REGION I
$N_{Re} = \left(\frac{\rho_l U_B r_0}{\mu_l}\right)$
△ TESTS 37, 39, 46, 47
○ TESTS 42, 43
● TESTS 48, 50, 52, 54

FIGURE 7

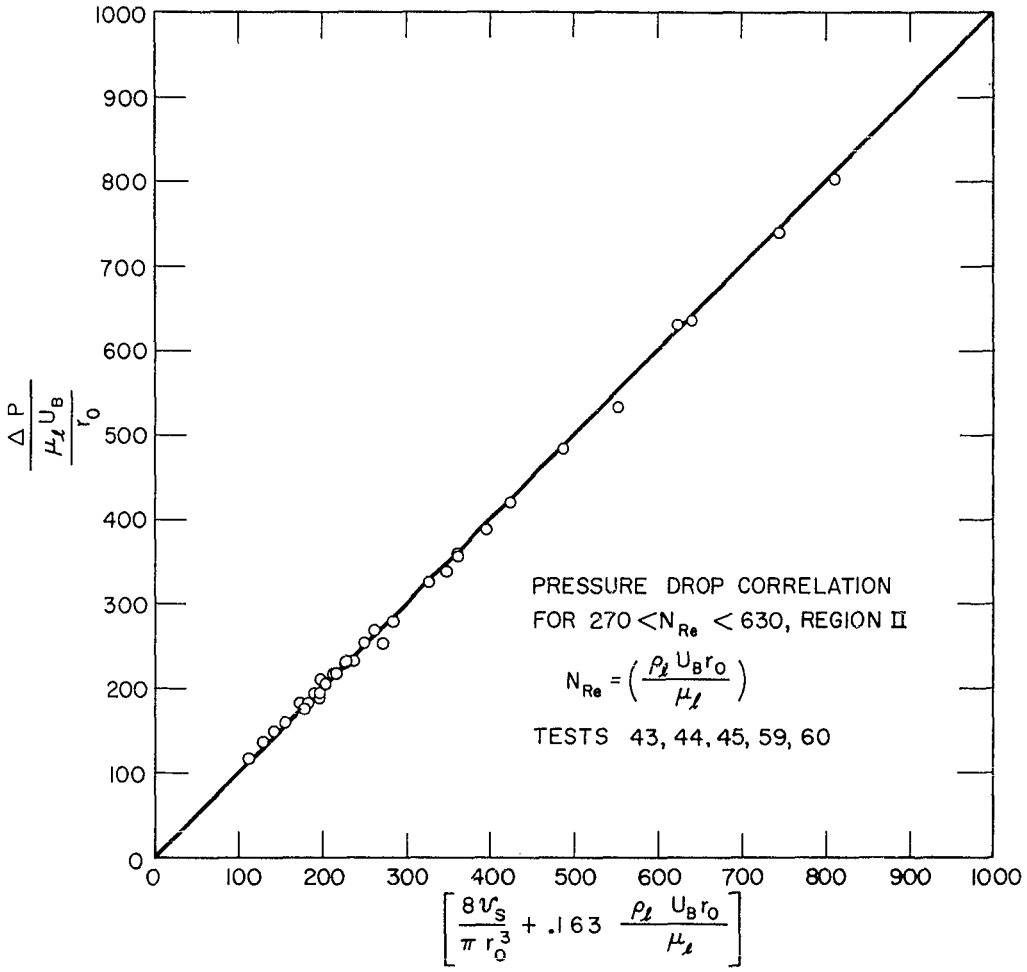
1000
900
800
700
600
500
400
300
200
100
0
0
100
200
300
400
500
600
700
800
900
1000
$\frac{\Delta P}{\mu_\ell U_B / r_o}$
$\left[\frac{8 v_s}{\pi r_o^3} + .163 \frac{\rho_\ell U_B r_o}{\mu_\ell}\right]$
PRESSURE DROP CORRELATION
FOR $270 < N_{Re} < 630$, REGION II
$N_{Re} = \left(\frac{\rho_\ell U_B r_o}{\mu_\ell}\right)$
TESTS 43, 44, 45, 59, 60

FIGURE 8

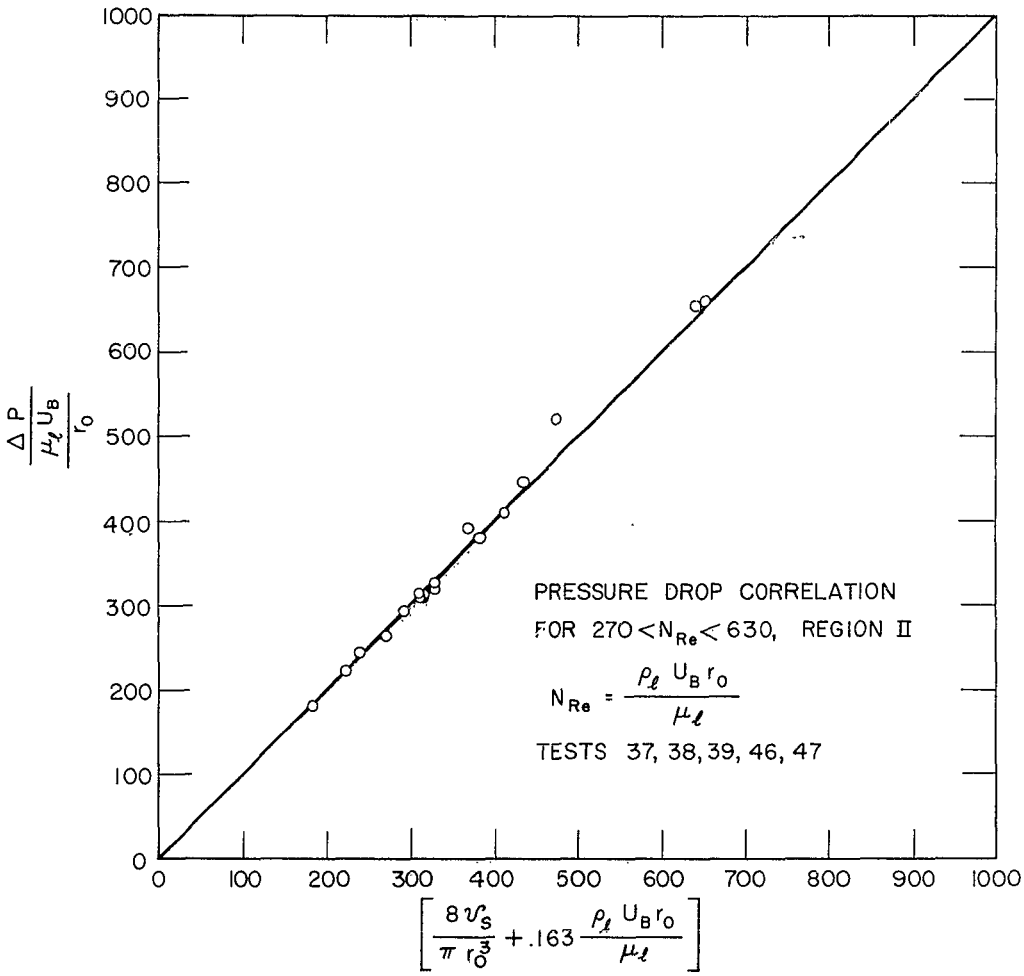
1000
900
800
700
600
500
400
300
200
100
0
0
100
200
300
400
500
600
700
800
900
1000
$\frac{\Delta P}{\mu_\ell \frac{U_B}{r_o}}$
PRESSURE DROP CORRELATION
FOR $270 < N_{Re} < 630$, REGION II
$N_{Re} = \frac{\rho_\ell U_B r_o}{\mu_\ell}$
TESTS 37, 38, 39, 46, 47
$\left[\frac{8 v_s}{\pi r_o^3} + .163 \frac{\rho_\ell U_B r_o}{\mu_\ell}\right]$

FIGURE 9

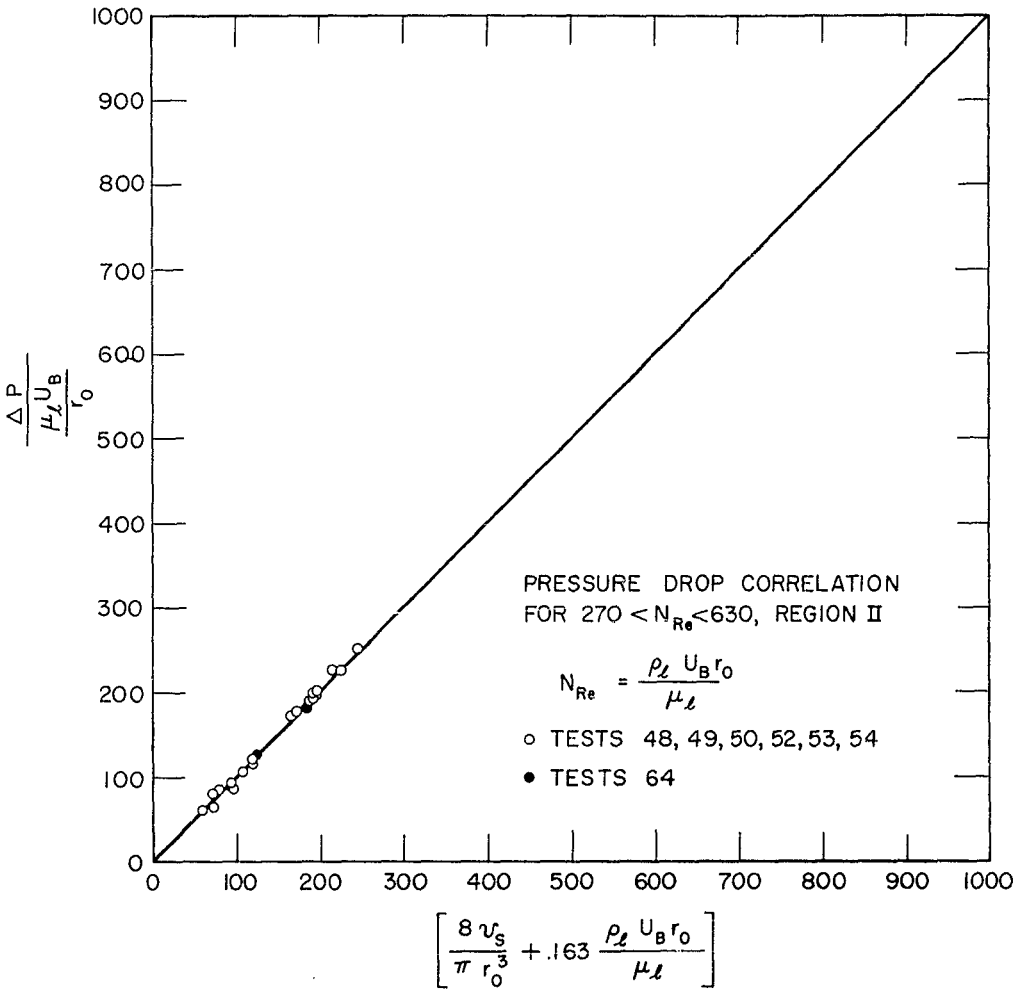
1000
900
800
700
600
500
400
300
200
100
0
0
100
200
300
400
500
600
700
800
900
1000
$\frac{\Delta P}{\mu_\ell \frac{U_B}{r_o}}$
$\left[\frac{8 v_s}{\pi r_o^3} + .163 \frac{\rho_\ell U_B r_o}{\mu_\ell}\right]$
PRESSURE DROP CORRELATION
FOR $270 < N_{Re} < 630$, REGION II
$N_{Re} = \frac{\rho_\ell U_B r_o}{\mu_\ell}$
○ TESTS 48, 49, 50, 52, 53, 54
● TESTS 64

FIGURE 10

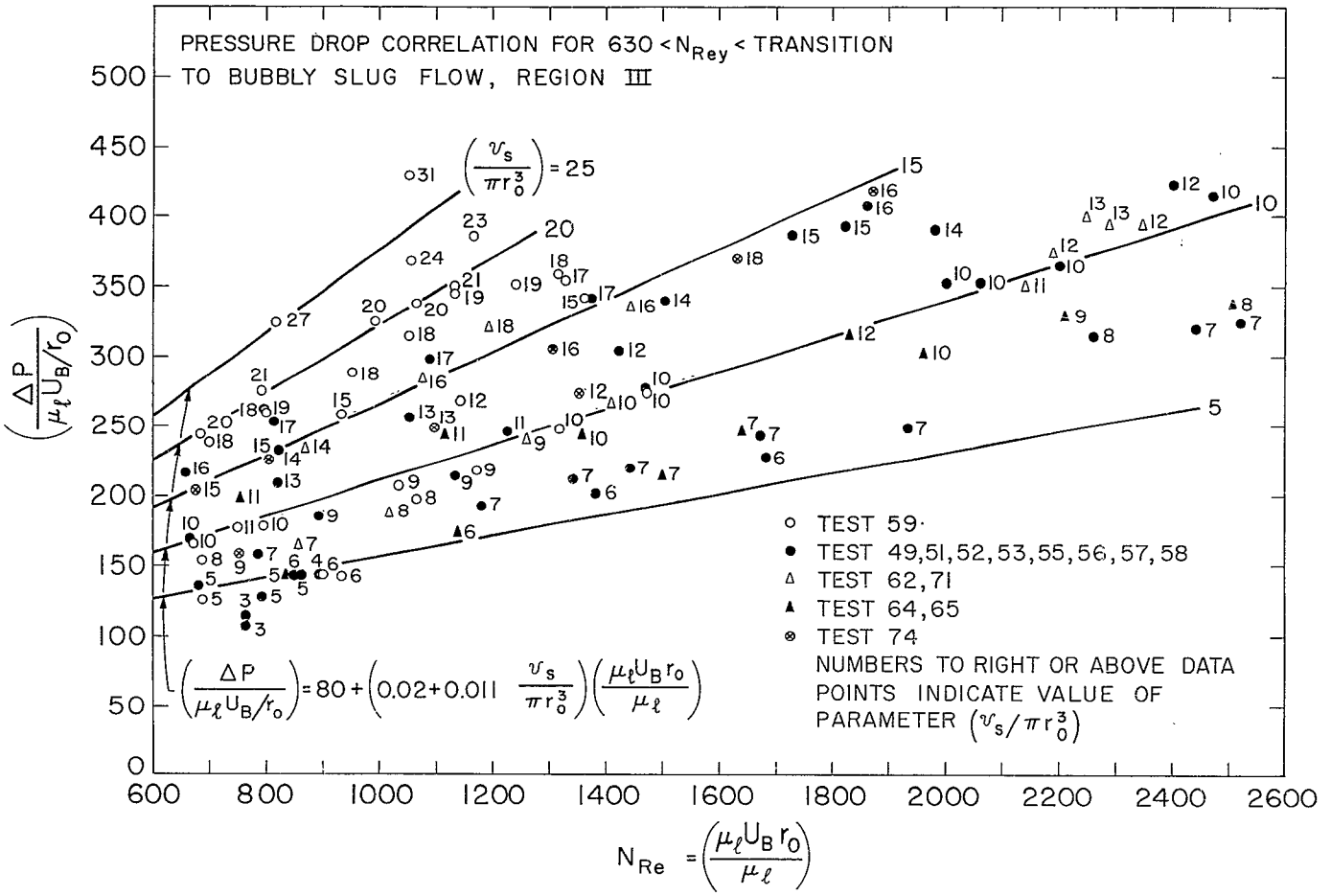
PRESSURE DROP CORRELATION FOR 630 < N_{Rey} < TRANSITION TO BUBBLY SLUG FLOW, REGION III
$\left(\frac{\Delta P}{\mu_\ell U_B / r_0}\right)$
$N_{Re} = \left(\frac{\mu_\ell U_B r_0}{\mu_\ell}\right)$
$\left(\frac{v_s}{\pi r_0^3}\right) = 25$
20
15
10
5
$\left(\frac{\Delta P}{\mu_\ell U_B / r_0}\right) = 80 + \left(0.02 + 0.011 \frac{v_s}{\pi r_0^3}\right)\left(\frac{\mu_\ell U_B r_0}{\mu_\ell}\right)$
TEST 59
TEST 49,51,52,53,55,56,57,58
TEST 62,71
TEST 64,65
TEST 74
NUMBERS TO RIGHT OR ABOVE DATA POINTS INDICATE VALUE OF PARAMETER $\left(v_s/\pi r_0^3\right)$

FIGURE 11

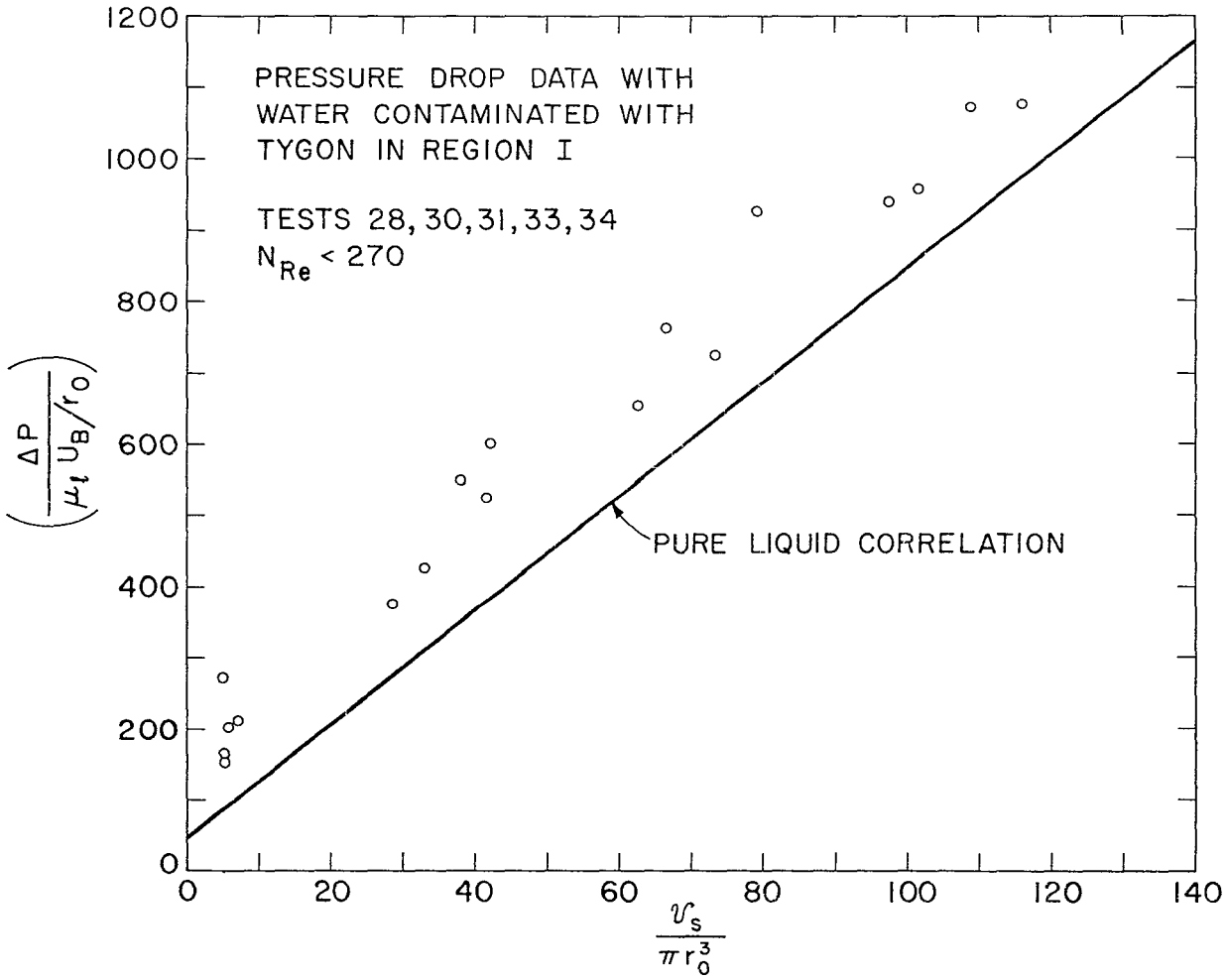
PRESSURE DROP DATA WITH
WATER CONTAMINATED WITH
TYGON IN REGION I
TESTS 28, 30, 31, 33, 34
$N_{Re} < 270$
PURE LIQUID CORRELATION
$\left(\frac{\Delta P}{\mu_t U_B / r_0}\right)$
$\frac{v_s}{\pi r_0^3}$
0
200
400
600
800
1000
1200
0
20
40
60
80
100
120
140

FIGURE 12

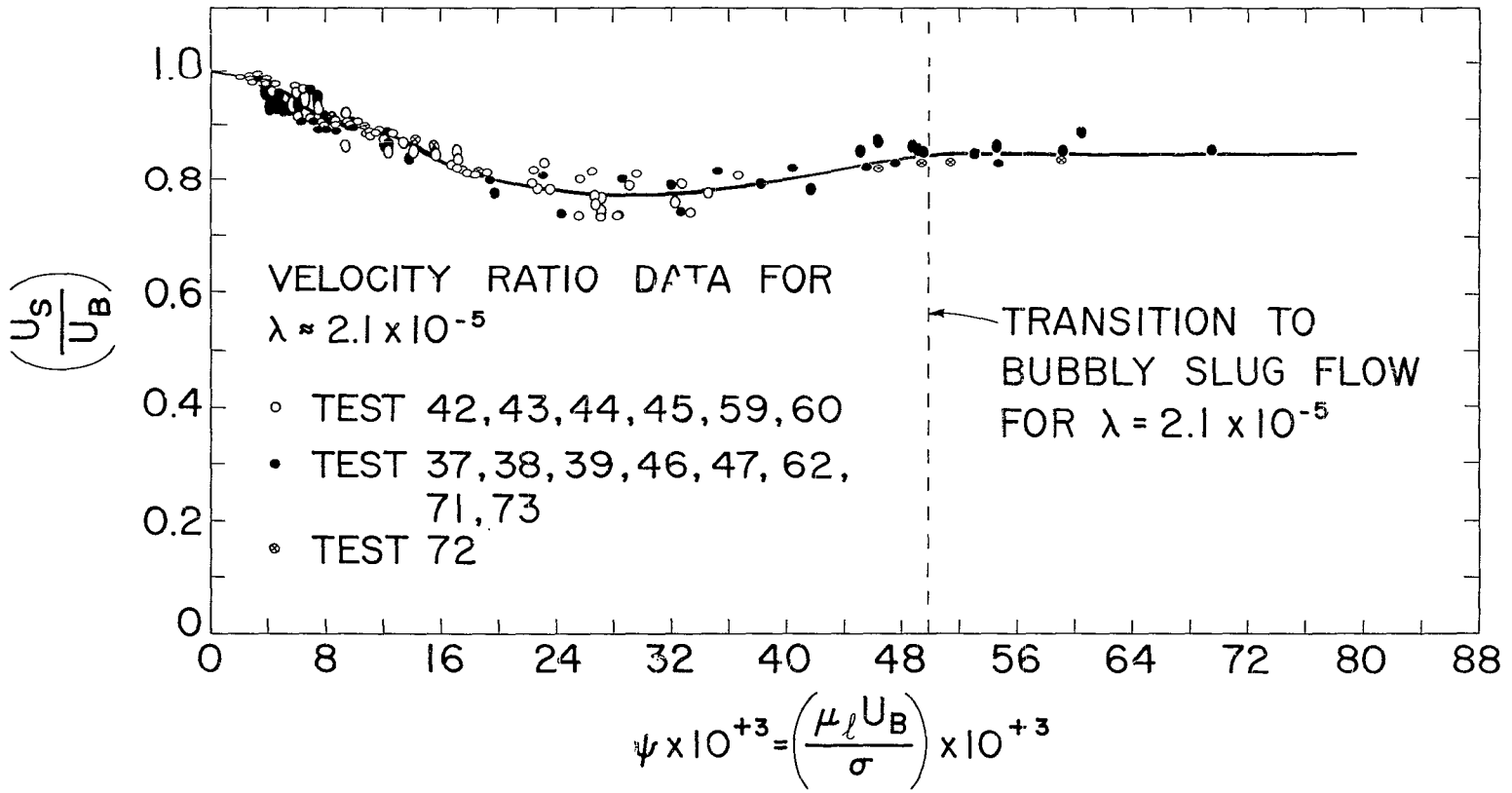
1.0
0.8
0.6
0.4
0.2
0
$\frac{U_S}{U_B}$
VELOCITY RATIO DATA FOR
$\lambda \approx 2.1 \times 10^{-5}$
○ TEST 42,43,44,45,59,60
• TEST 37,38,39,46,47,62, 71,73
⊗ TEST 72
TRANSITION TO BUBBLY SLUG FLOW FOR $\lambda = 2.1 \times 10^{-5}$
0 8 16 24 32 40 48 56 64 72 80 88
$\psi \times 10^{+3} = \left(\frac{\mu_\ell U_B}{\sigma}\right) \times 10^{+3}$

FIGURE 13

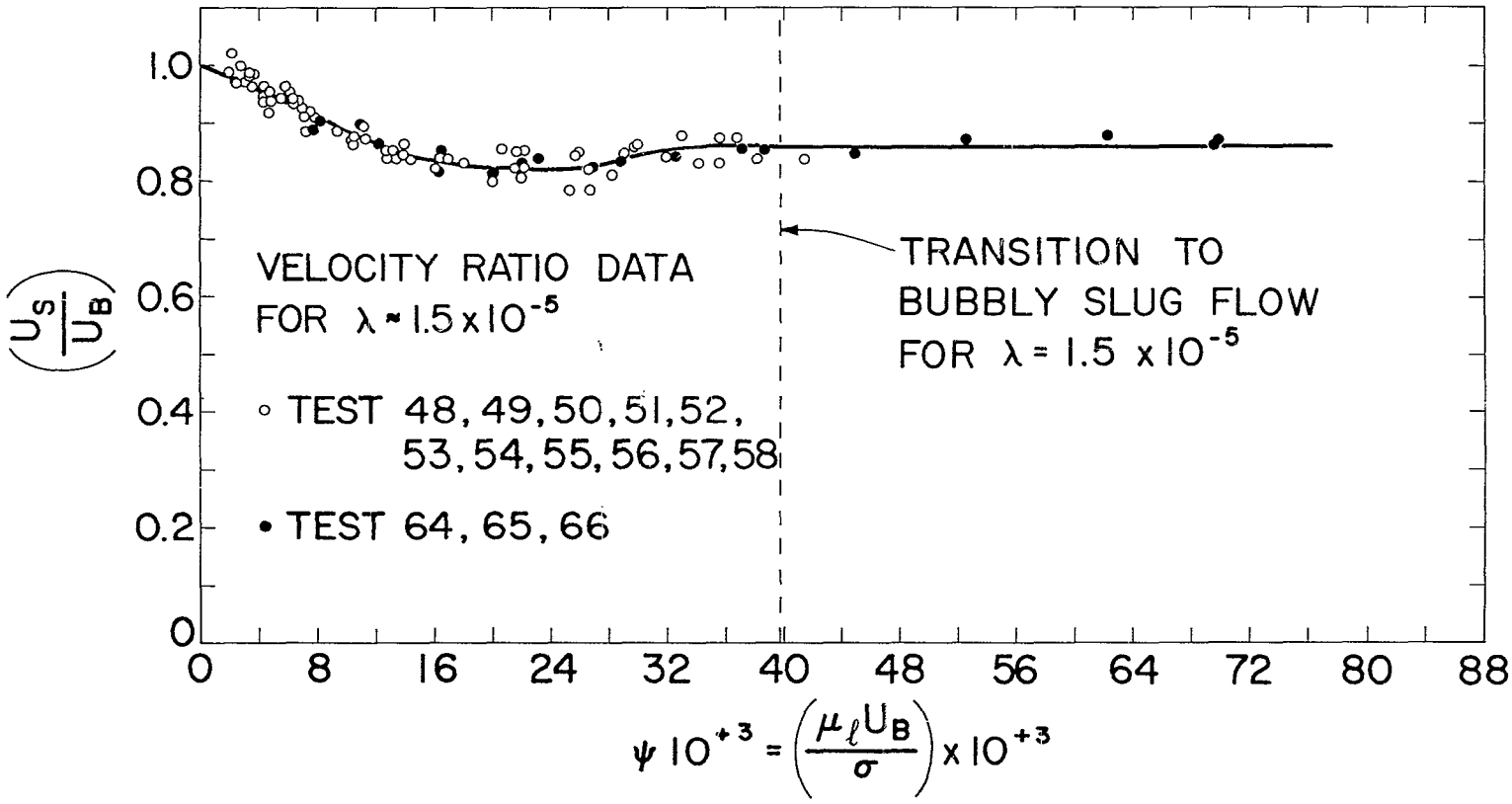
1.0
0.8
0.6
0.4
0.2
0
$\frac{U_S}{U_B}$
VELOCITY RATIO DATA
FOR $\lambda \approx 1.5 \times 10^{-5}$
○ TEST 48, 49, 50, 51, 52,
53, 54, 55, 56, 57, 58
• TEST 64, 65, 66
TRANSITION TO
BUBBLY SLUG FLOW
FOR $\lambda = 1.5 \times 10^{-5}$
0
8
16
24
32
40
48
56
64
72
80
88
$\psi\, 10^{+3} = \left(\frac{\mu_\ell U_B}{\sigma}\right) \times 10^{+3}$

FIGURE 14

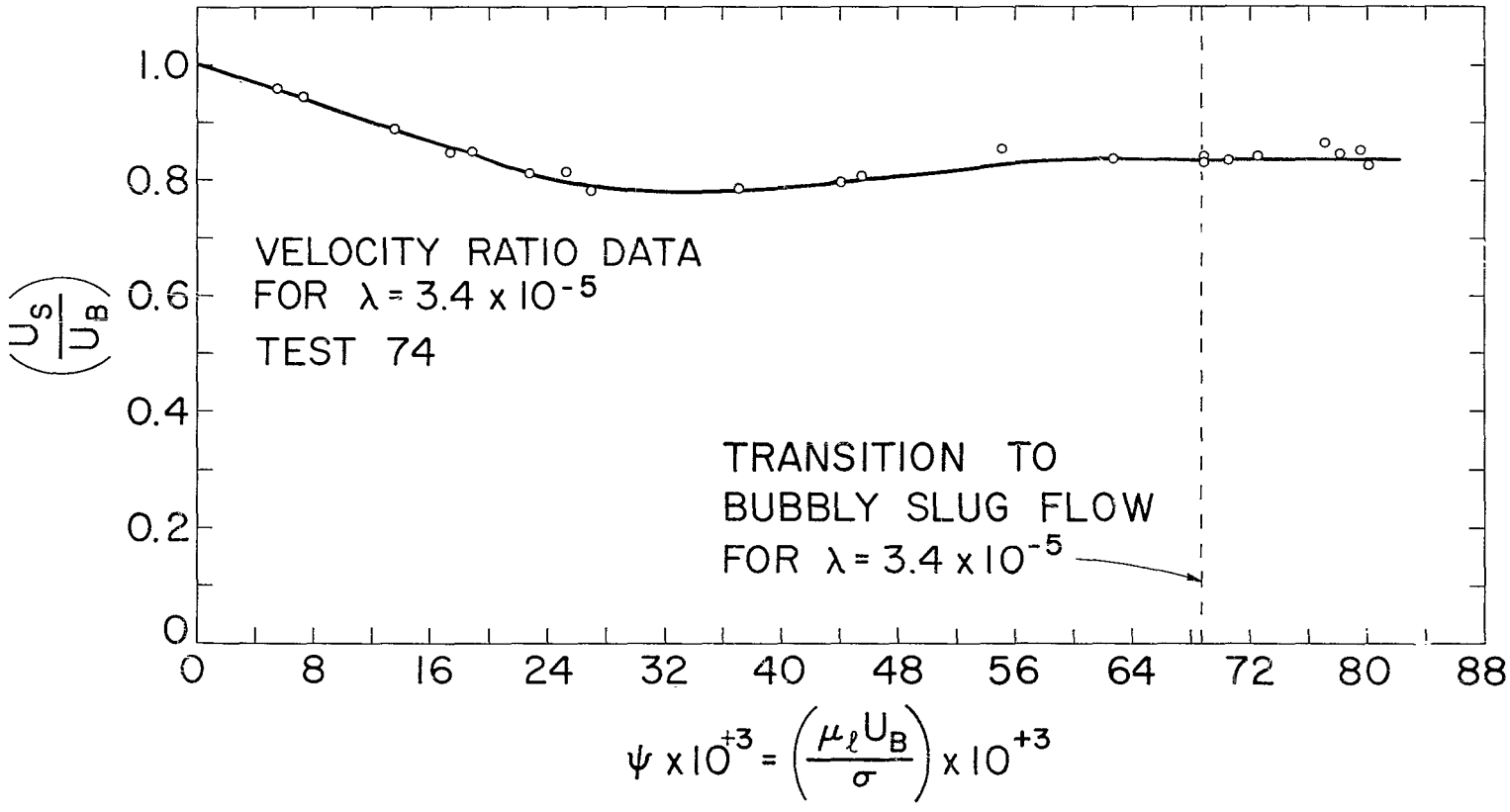
1.0
0.8
0.6
0.4
0.2
0
$\left(\frac{U_S}{U_B}\right)$
VELOCITY RATIO DATA
FOR $\lambda = 3.4 \times 10^{-5}$
TEST 74
TRANSITION TO
BUBBLY SLUG FLOW
FOR $\lambda = 3.4 \times 10^{-5}$
0
8
16
24
32
40
48
56
64
72
80
88
$\psi \times 10^{+3} = \left(\frac{\mu_\ell U_B}{\sigma}\right) \times 10^{+3}$

FIGURE 15

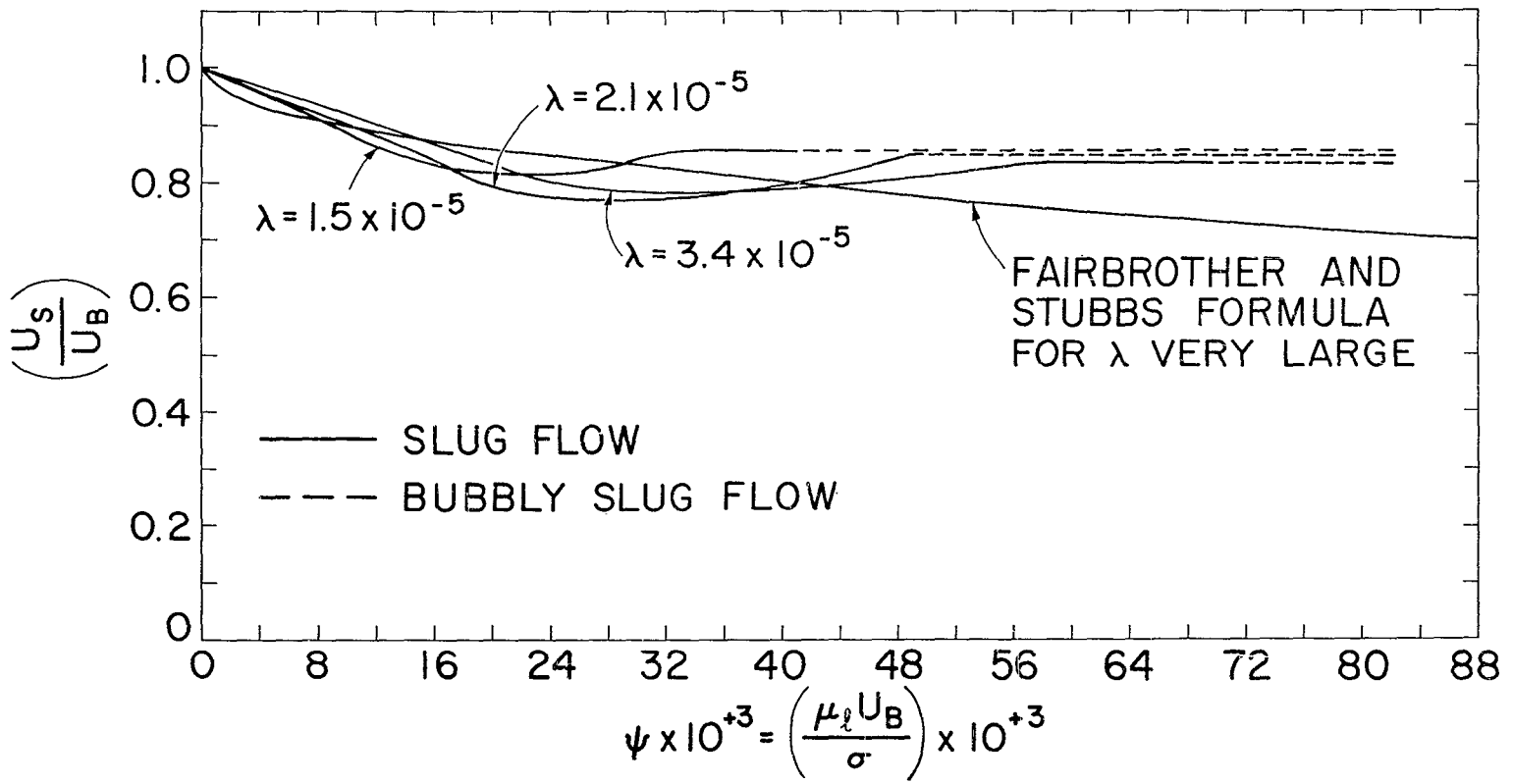

VELOCITY RATIO CORRELATION

FIGURE 16

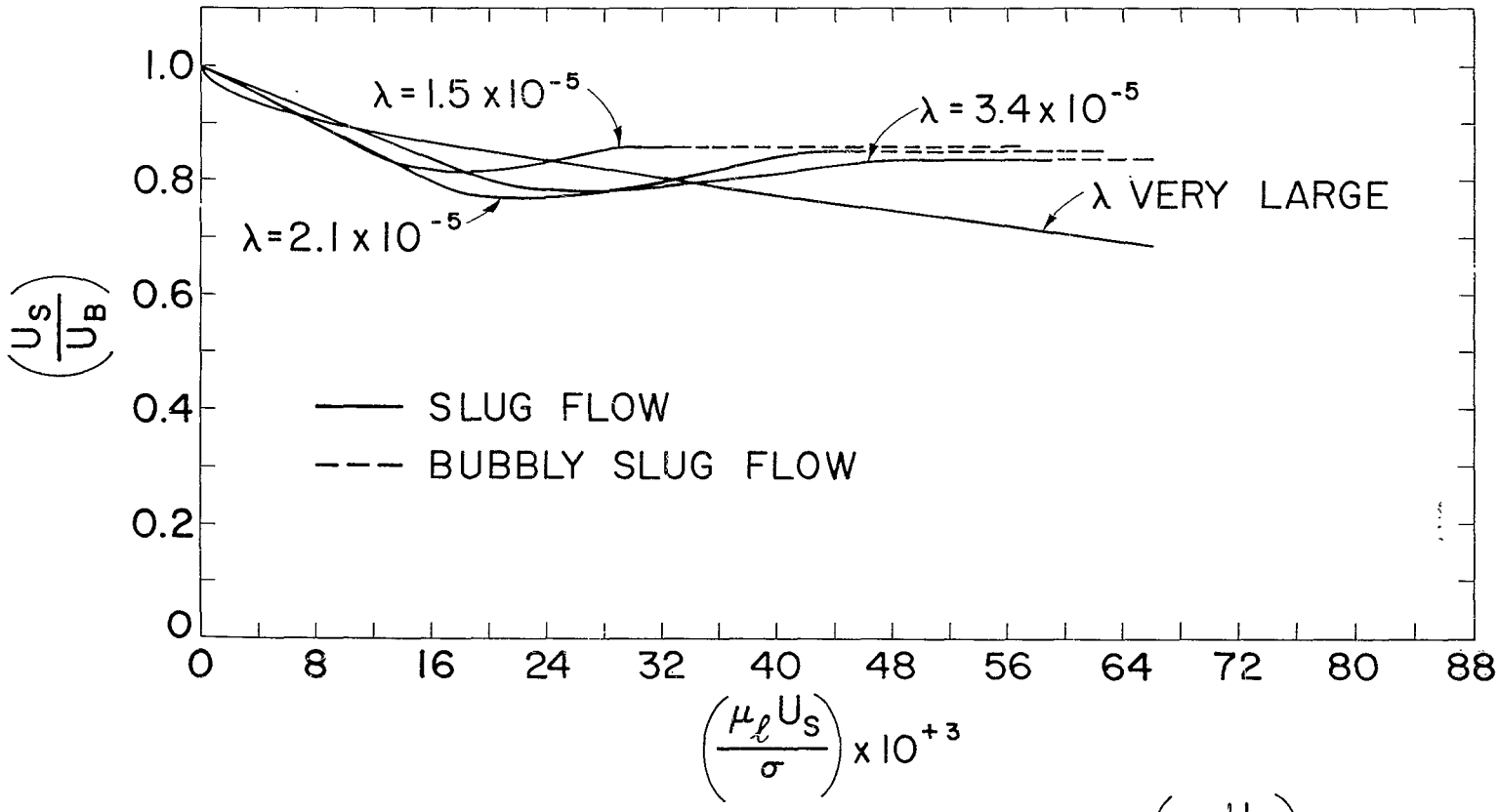

VELOCITY RATIO AS A FUNCTION OF $\left(\frac{\mu_\ell U_S}{\sigma}\right)$

FIGURE 17

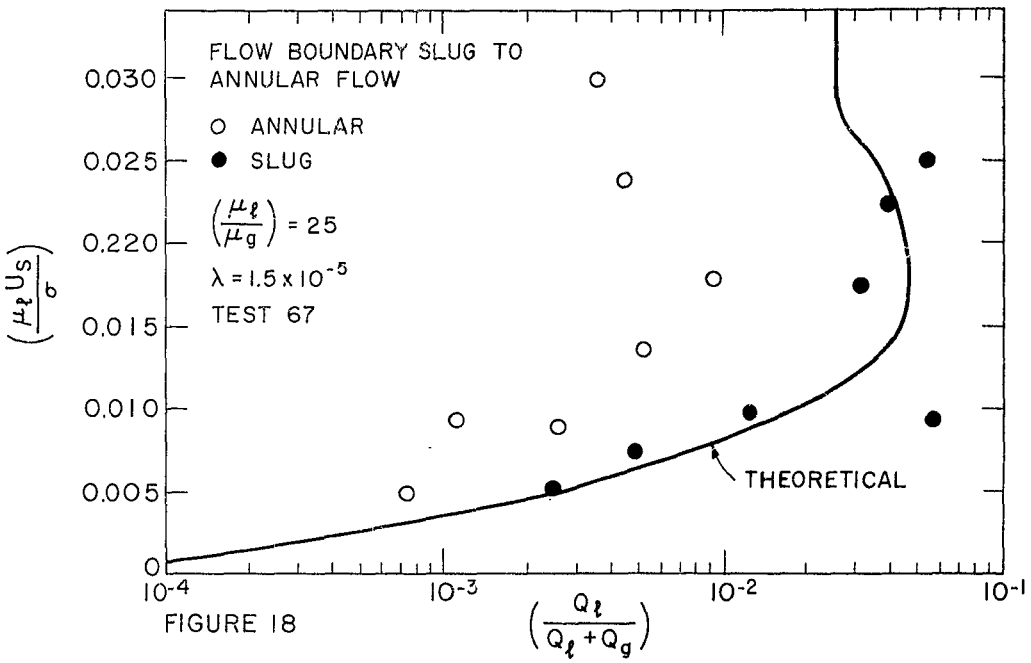

FIGURE 18

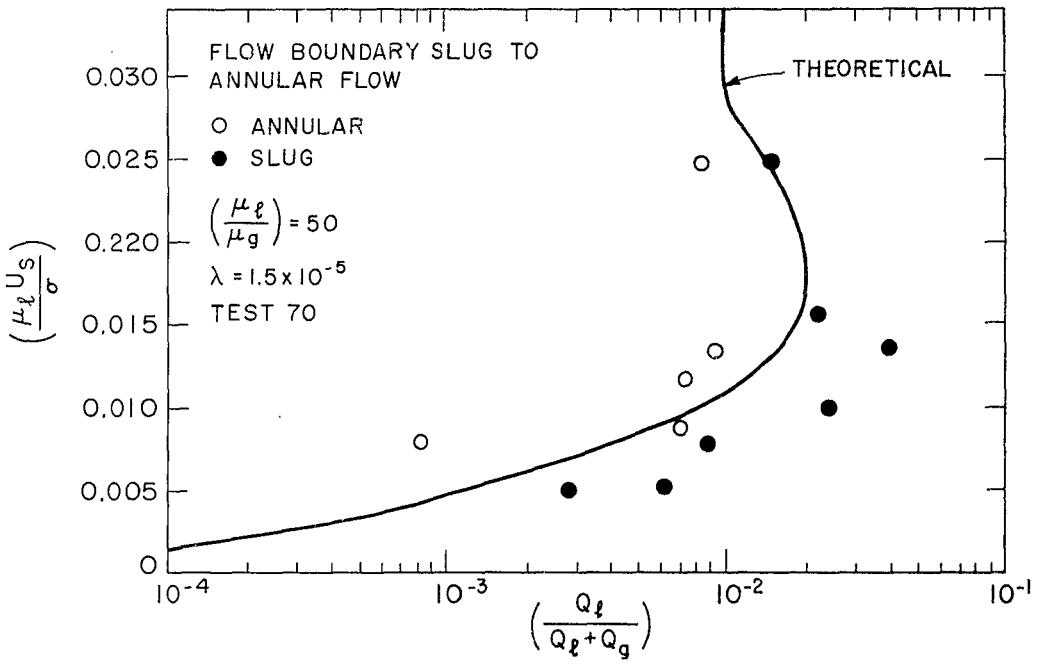

FIGURE 19

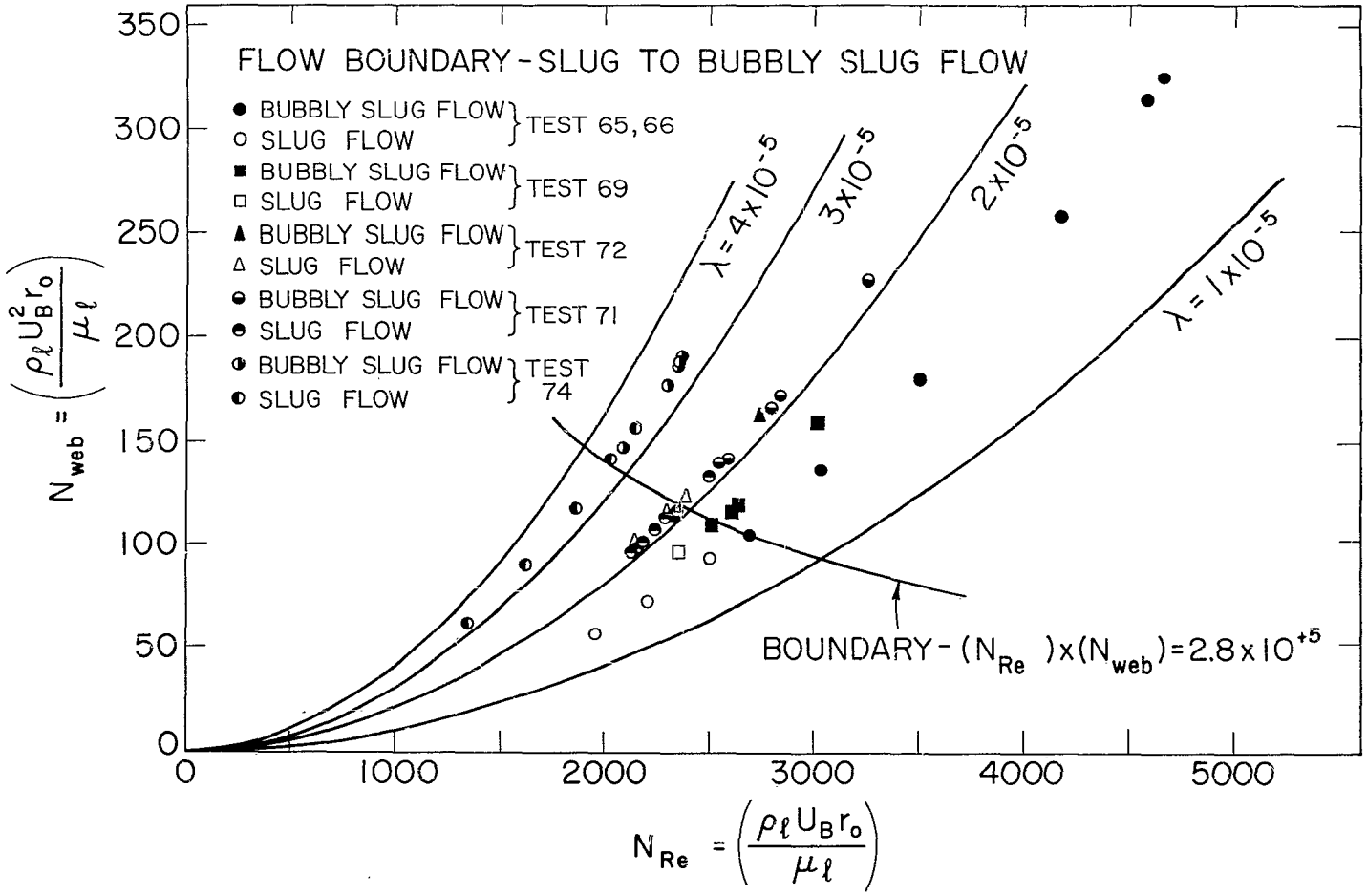
FLOW BOUNDARY - SLUG TO BUBBLY SLUG FLOW
BUBBLY SLUG FLOW
SLUG FLOW
TEST 65,66
BUBBLY SLUG FLOW
SLUG FLOW
TEST 69
BUBBLY SLUG FLOW
SLUG FLOW
TEST 72
BUBBLY SLUG FLOW
SLUG FLOW
TEST 71
BUBBLY SLUG FLOW
SLUG FLOW
TEST 74
λ = 4x10⁻⁵
3x10⁻⁵
2x10⁻⁵
λ = 1x10⁻⁵
BOUNDARY - (N_Re)x(N_web)=2.8x10⁺⁵
N_web = (ρ_l U_B² r_o / μ_l)
N_Re = (ρ_l U_B r_o / μ_l)
0
50
100
150
200
250
300
350
0
1000
2000
3000
4000
5000

FIGURE 20

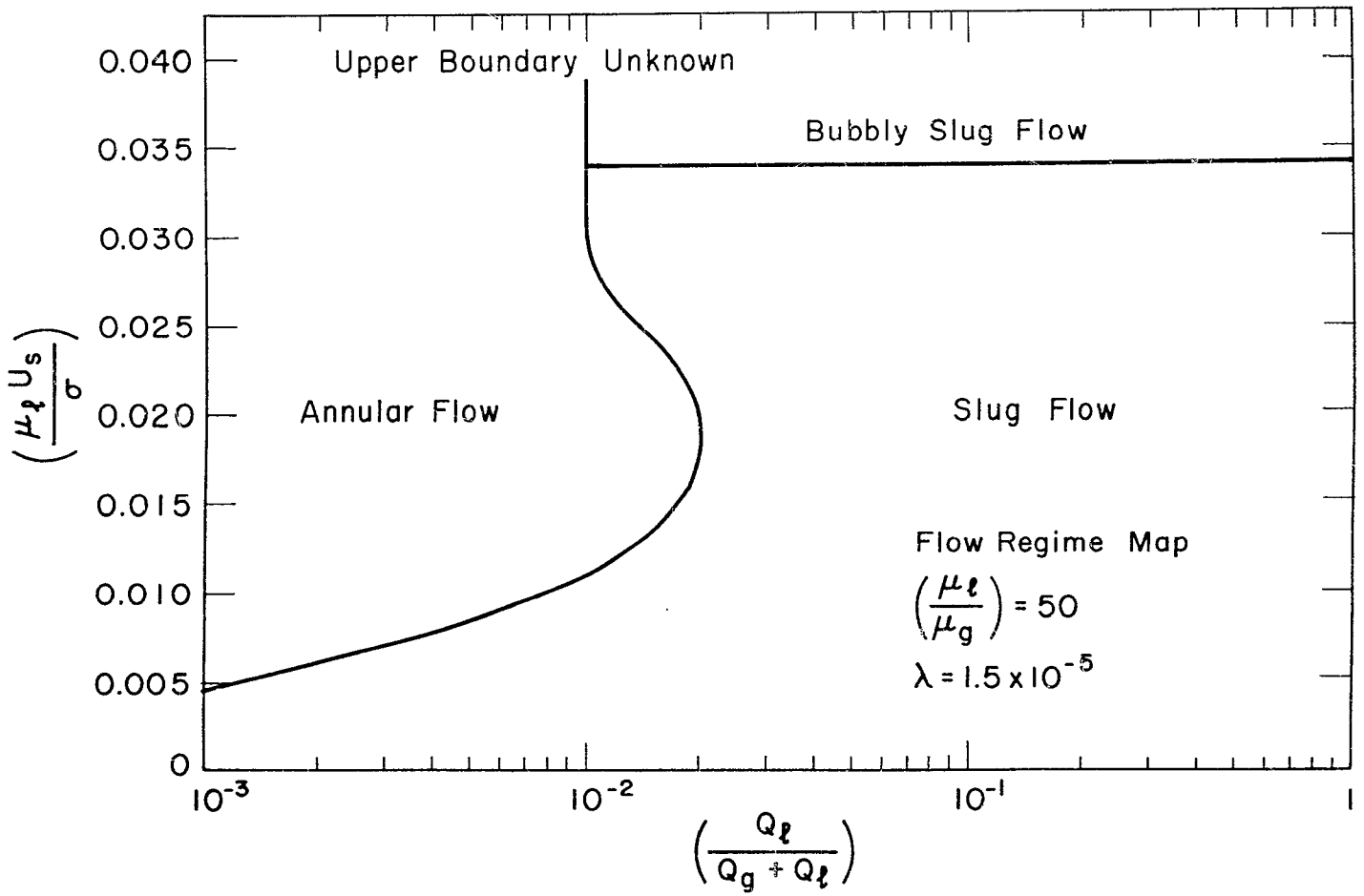
Upper Boundary Unknown
Bubbly Slug Flow
Annular Flow
Slug Flow
Flow Regime Map
$\left(\frac{\mu_\ell}{\mu_g}\right) = 50$
$\lambda = 1.5 \times 10^{-5}$
0.040
0.035
0.030
0.025
0.020
0.015
0.010
0.005
0
10^{-3}
10^{-2}
10^{-1}
1
$\left(\frac{\mu_\ell U_s}{\sigma}\right)$
$\left(\frac{Q_\ell}{Q_g + Q_\ell}\right)$

FIGURE 21

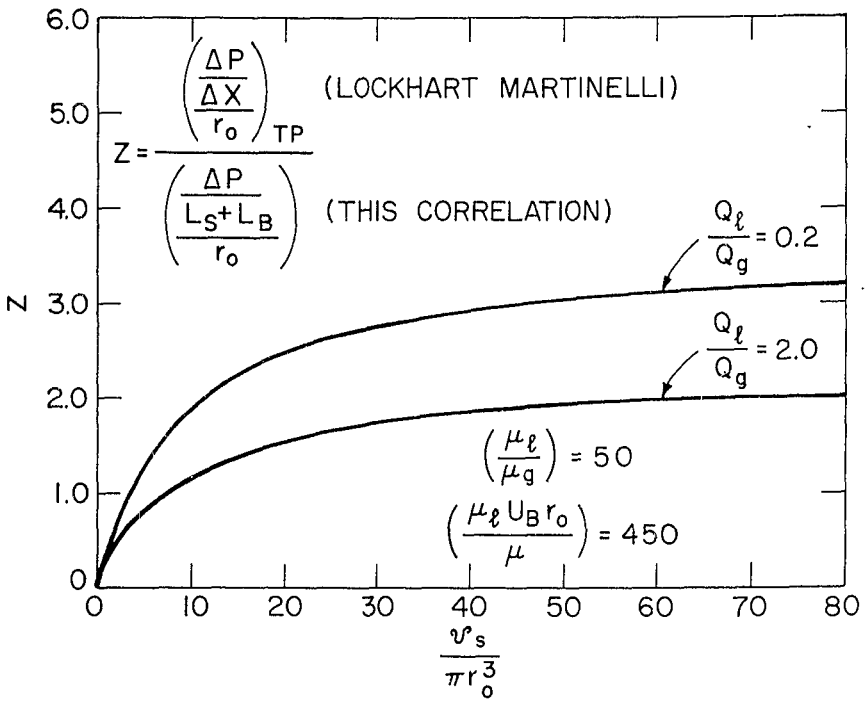

COMPARISON OF LOCKHART MARTINELLI PRESSURE-DROP TO THIS CORRELATION

FIGURE 22

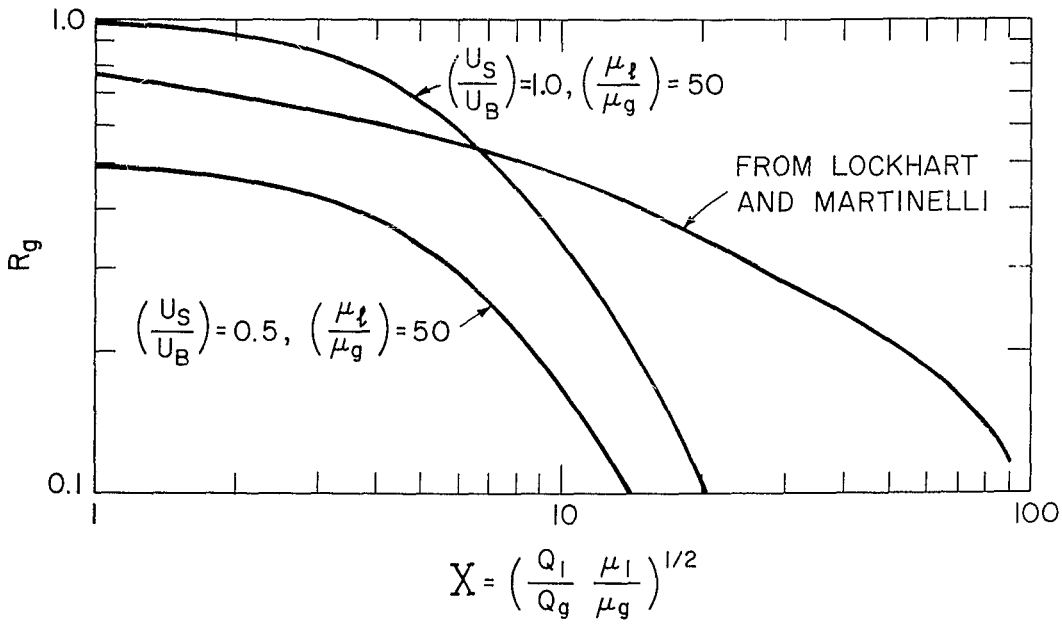

COMPARISON OF VOID VOLUME TO LOCKHART AND MARTINELLI

FIGURE 23